# EMBRY-RIDDLE
## Aeronautical University™
### SCHOLARLY COMMONS

Publications

2-16-2005

# The Chromospheric Activity and Ages of M Dwarf Stars in Wide Binary Systems

Nicole M. Silvesteri
*Department of Astronomy, University of Washington*, nms@astro.washington.edu

T. D. Oswalt
*Florida Institute of Technology*, oswaltt1@erau.edu

Suzanne L. Hawley
*Department of Astronomy, University of Washington*, slh@astro.washington.edu

Follow this and additional works at: https://commons.erau.edu/publication

Part of the Stars, Interstellar Medium and the Galaxy Commons

## Scholarly Commons Citation

# THE CHROMOSPHERIC ACTIVITY AND AGES OF M DWARF STARS IN WIDE BINARY SYSTEMS[1]

Nicole M. Silvestri[2], Suzanne L. Hawley[2], and Terry D. Oswalt[3]

*Accepted for publication in the Astronomical Journal, May 2005*

## ABSTRACT

We investigate the relationship between age and chromospheric activity for 139 M dwarf stars in wide binary systems with white dwarf companions. The age of each system is determined from the cooling age of its white dwarf component. The current limit for activity-age relations found for M dwarfs in open clusters is 4 Gyr. Our unique approach to finding ages for M stars allows for the exploration of this relationship at ages older than 4 Gyr. The general trend of stars remaining active for a longer time at later spectral type is confirmed. However, our larger sample and greater age range reveals additional complexity in assigning age based on activity alone. We find that M dwarfs in wide binaries older than 4 Gyr depart from the log-linear relation for clusters and are found to have activity at magnitudes, colors and masses which are brighter, bluer and more massive than predicted by the cluster relation. In addition to our activity-age results, we present the measured radial velocities and complete space motions for 161 white dwarf stars in wide binaries.

*Subject headings:* stars: activity — stars: ages — stars: binaries — stars: low-mass — stars: white dwarfs — techniques: spectroscopic

## 1. INTRODUCTION

The study of stellar activity has long been restricted to observed features on the surface of the Sun and to bright solar-type stars (Byrne 1993; Byrne & Doyle 1990). Studies conducted by, among others, Wilson (1966), Skumanich (1972), and Noyes et al. (1984) showed a link between activity in solar-type stars and the stellar rotation rate. An $\alpha\Omega$ dynamo driven by differential rotation at the radiative-convective boundary layer is thought to be the primary driver behind stellar activity in F, G, K, and early M stars. It is also believed to be responsible for the heating of the stellar chromosphere and corona as well as the production of star spots, flares, and prominences.

Recently, the study of stellar activity has been extended to include the entire M dwarf sequence. At first glance the magnetic activity observed in these low mass stars appears similar to that found in solar type stars, and in some cases is particularly strong. The dynamo generation mechanism must be different however, as these stars should be fully convective and therefore lacking the radiative-convective boundary layer responsible for magnetic dynamo generation in more massive

stars (cf. Pettersen & Hawley 1989; O'Neal, Neff, & Saar 1998; Ding & Fang 2001; Martín & Ardila 2001).

Due to their slow burning of core hydrogen, M dwarfs that formed at the birth of the Galaxy are still on the main sequence and therefore retain information from the Galaxy's earliest epochs of star formation. In this study we investigate the relationship between magnetic activity and age for M dwarfs, with the goal of developing an age-activity relation that can be used to determine ages for this important and ubiquitous population.

Stellar age is one of the most difficult properties of a star to determine. Skumanich (1972) showed that chromospheric activity and age are related for solar-type stars by:

$$F(\text{Ca K}) = At^{-1/2}, \qquad (1)$$

where $F(\text{Ca K})$ is the equivalent width of the Ca II K chromospheric emission line (in Å), $A$ is a constant, and $t$ is the age of the star (in years). The common explanation for this effect is that as the star ages, its rotation slows due to mass and angular momentum loss. This leads to a weakening of the internal rotationally-driven dynamo, causing a decrease in magnetic heating and hence chromospheric activity. Calibration of the chromospheric activity−age relation for F, G, and K stars has been carried out by Barry (1988) and Soderblom, Duncan, & Johnson (1991). However, a similar relation does not appear to hold for the M dwarfs. Stauffer et al. (1991) originally showed that all stars redder (lower temperature, lower mass) than a given $R - I$ color had Hα emission in the Pleiades and Hyades clusters. The color at the "Hα limit" was bluer, corresponding to a higher mass where activity still occurred, in the younger cluster. This result led to the speculation that both mass and age affect the Hα limit. A subsequent study of six open clusters (IC2602, IC2391, NGC2516, Pleiades, Hyades, and M67 Hawley, Reid, & Tourtellot 2000, hereafter HRT) showed that there was a linear re-

the log(age) of the cluster. The $V - I$ color is directly related to the atmospheric temperature and therefore the mass of a main sequence M dwarf. The relationship was calibrated only for relatively young M dwarfs with ages < 4 Gyr (the age of M67, the oldest open cluster in their study). Thus, HRT confirmed that activity in M dwarfs is a function of age at a given mass (or alternatively mass at a given age), quite unlike the rotationally-dependent Skumanich relation for F−K stars, which appears to be independent of mass. The HRT age-activity relationship was used by Gizis, Reid, & Hawley (2002) to constrain the ages of brown dwarf stars in binaries with M dwarf companions and to study the star formation history of the Galactic disk.

Unfortunately, it is not yet feasible to spectroscopically determine the activity levels of older M dwarfs in either open or globular clusters, because the clusters are faint and distant, making the observations difficult even on the largest telescopes. Therefore, the current activity−age relation determined with the use of clusters only allows for the sampling of stars formed well after the earliest epochs of star formation in the Galaxy. Further progress in pinning down the old, low mass end of the M dwarf chromospheric activity−age relation must therefore come from another method.

Here we describe our analysis of a sample of ∼ 200 spectroscopically identified M dwarf stars in common proper motion binary (CPMB) systems with white dwarf (WD) companions. The age of the system is determined from the cooling age of the companion WD, assuming the WD and M dwarf are coeval. The WD ages are accurate to roughly 25% (or better if the mass of the WD is known), comparable to the accuracy determined from the ages of clusters. Since many binaries in our sample have ages well beyond the present 4 Gyr cluster limit, this allows us to examine the activity−age relation for much older M dwarfs. Concurrently, our sample provides a significant amount of new data on WD stars in binary systems.

Using the spectra of the M dwarfs, we determine the spectral types (masses) and from the photometry of the WDs we determine the age of each pair in which activity is observed. In addition, we determine the radial velocities of the M stars and, since proper motions are known, the complete space motions for all systems in the observed sample. This allows us to examine the kinematics and provides an independent indicator of population membership.

The paper is organized as follows: In §2 we introduce the sample and selection criteria, and describe the observations, data reduction and determination of M dwarf atmospheric parameters. Our method for estimating ages of the WDs using atmospheric and evolutionary models is presented in §3. In §4 we examine the spectroscopic and photometric properties of the active M dwarfs and present the final activity−age results for the sample. We discuss the kinematics of the sample and the implications of these results in §5, building on the earlier work in Silvestri, Oswalt, & Hawley (2002). Our conclusions are summarized in §6.

## 2. SAMPLE SELECTION AND OBSERVATIONS

Luyten (1963, 1969, 1974, 1979) and Giclas, Burnham, & Thomas (1971, 1978) first identified a number of over 500 wide binary systems in

several proper motion-selected surveys from the original Palomar Observatory Sky Survey (POSS) plates and the photographic plates from Lowell Observatory. The Luyten−Giclas CPMB systems have relatively wide orbital separations ($\langle a \rangle \sim 10^3$ A.U., Oswalt et al. 1993). Unlike close binary systems, these wide pairs are not influenced by mass exchange and evolve essentially as two single stars. The stars that make up a CPMB (or multiple component) system originally evolved from the same molecular cloud (Boss 1987, 1988; Pringle 1989) and are therefore taken to be coeval. Of particular interest to our study are those CPMBs which contain one WD and one main sequence M dwarf star (we will refer to these systems as WD+dM pairs). Among these pairs are some with very faint and cool (hence old) WD stars (Liebert, Dahn, & Monet 1988; Oswalt et al. 1996), which are particularly useful for setting a firm lower limit to the age of the Galaxy. Here we also show that they are useful for extending the age range of the age-activity relationship.

A subset of 196 systems was selected for observation (see Table 1). The sole selection criterion was that the system must contain spectroscopically identified WD and M dwarf stars. Low resolution spectra (7−15 Å pixel$^{-1}$, Oswalt, Hintzen, & Luyten 1988; Oswalt et al. 1991, 1993) were used to confirm the rough spectral type of each CPMB component. Of the 196 systems, 189 are binary (WD+dM) and seven are triple systems (one WD+dM+dK, one WD+dM+dG, three WD+dM+dM, and two WD+WD+dM). This gives a total of 199 M dwarf stars with at least one WD companion. Table 1 lists all 196 system names as assigned by Luyten in column 1, their R.A. and Decl. (coordinates are for equinox 1950; columns 2 & 3), the $V$ magnitude and original low resolution spectroscopic identification (columns 4-7), the site, date, and exposure time at which the object was observed (columns 8-10). Columns 11-14 list the proper motion, direction of proper motion (measured east of north), position angle (centered on the primary measured east of north), and the separation of the components, respectively.

The biases in our sample, imposed primarily by the sampling area, proper motion ($\mu$) criteria, and limiting apparent magnitude (in this case photographic magnitude, $m_{\rm pg}$) of the original surveys, are well understood (see Oswalt & Smith 1995; Smith & Oswalt 1995; Oswalt et al. 1996; Wood & Oswalt 1998). Our sample includes objects north of declination $-60°$ excluding the most dense regions of the Galactic plane (|b| < 15°). It thus includes ∼ 65% of the visible sky (Dawson 1986). The Luyten−Giclas binaries are restricted to 0.1 ≤ $\mu$ ≤ 2″.5 yr$^{-1}$ (La Bonte 1970), a limit based solely on Luyten's ability to discern motion between the original and retake plates of the POSS. The magnitudes of the CPMBs are $m_{\rm pg} \leq 20$, i.e. down to the rough magnitude limit of the POSS blue plate. It should also be noted that because Luyten avoided listing pairs that he knew had already been discovered by Giclas, the latter need to be included in any sample where completeness is important.

### 2.1. *Spectroscopic Observations*

The northern portion of the sample was observed spectroscopically during 32 half-nights on the ARC 3.5-m telescope at APO. Observations were performed on the

($\sim 2$ Å/pixel) with a $1''.5$ slit. With this setup, slits were centered at 6700 Å (red) and 4600 Å (blue) yielding wavelength coverage of $\sim$6000-7500 Å and $\sim$4000-5200 Å, respectively. An additional three full nights of observing time on the CTIO 4-m Blanco telescope were used to observe the systems which could not be seen from the northern hemisphere. Observations were performed with the R$-$C Spectrograph in medium-resolution mode ($\sim$ 4 Å/pixel) and a $1''.0$ slit. The grating tilt was centered at 6800 Å and covered a wavelength range of $\sim$3500-8500 Å. A condensed Journal of Observations is given in Table 2 where the first three columns give the UT date of the observing run followed by the site (column 4), the average seeing for the night (column 5), and some notes on the weather conditions (column 6).

We were unable to observe ten (40Eri$-$C, LP36$-$142, LP369$-$14, LP321$-$397, LP321$-$459, LP458$-$48, CD-51°13128, L427$-$61, LP411$-$22, and L573$-$109) of the 196 systems in our original sample (see Table 1). 40Eri$-$C was too close to its extremely bright companion to be observed. LP36$-$142, LP369$-$14, LP321$-$397, and LP321$-$459 were all too faint ($m_{pg} \geq 19.5$) to be observed in reasonable exposure times. The proper motion of the system LP458$-$49/48 has moved the M star (LP458$-$48) into the glare of a bright field star. CD$-$51°13128, L427$-$61, LP411$-$22, and L573$-$109 were not observed due to weather on the evenings on which they were slated for observation.

The data were reduced with standard $IRAF$[5] reduction procedures. In all cases, program objects were reduced with calibration data (bias, flat, arc, flux standard) taken on the same night. Data were bias subtracted and flat-fielded, and one-dimensional spectra were extracted using the standard aperture extraction method. A wavelength scale was determined for each target spectrum (including the flux and M dwarf standards) using He-Ne-Ar arc lamp calibrations. Flux standard stars were used to place the spectra on a calibrated flux scale. We emphasize that the final flux calibrations for the targets are only relative fluxes as most nights were not spectrophotometric.

After final reductions and close inspection of the individual spectra, we eliminated 28 M dwarfs from the final analysis because of insufficient signal to noise in the spectra. An additional 22 binaries were eliminated due to problems with the WD photometry as outlined in Smith (1997). This left 139 WD+dM binaries for final analysis in the activity$-$age relation in §4 and 161 M dwarf stars for the kinematics discussion in §5 (kinematics of the system are based on the M star so the 22 systems with poor WD photometry are included in this portion of the study).

### 2.2. *Spectroscopic Measurements*

The spectral types of the M dwarfs were determined by measuring the strength of Titanium Oxide (TiO) molecular features in the spectra, using flux ratios at strong bandheads as described in Reid, Hawley, & Gizis (1995). We used observations of M dwarf standards obtained at APO to calibrate the spectral type scale for our program as described in Kirkpatrick, Henry, & McCarthy

(1991) and Hawley et al. (2002), and found that our results agreed well with Reid, Hawley, & Gizis (1995). The uncertainty in M dwarf spectral type for this procedure is $\pm$ 0.5 spectral type at the APO resolution and $\pm$ 1.0 spectral type at the CTIO resolution. Figure 1 plots our measured TiO5 bandstrengths against the catalog spectral type. As displayed in the Figure the equation for the line of best fit is

$$\mathrm{Sp} = -11.17 \times \mathrm{TiO5} + 8.21, \sigma_{\mathrm{rms}} = \pm 0.52. \quad (2)$$

The relation adopted for this (TiO5, Sp) calibration by Reid, Hawley, & Gizis (1995) for their sample of 88 M dwarf standards defined by Kirkpatrick, Henry, & McCarthy (1991) is

$$\mathrm{Sp} = -10.775 \times \mathrm{TiO5} + 8.2, \sigma_{\mathrm{rms}} = \pm 0.5. \quad (3)$$

Clearly, the relation is in good agreement with the larger sample of standards from Reid, Hawley, & Gizis (1995).
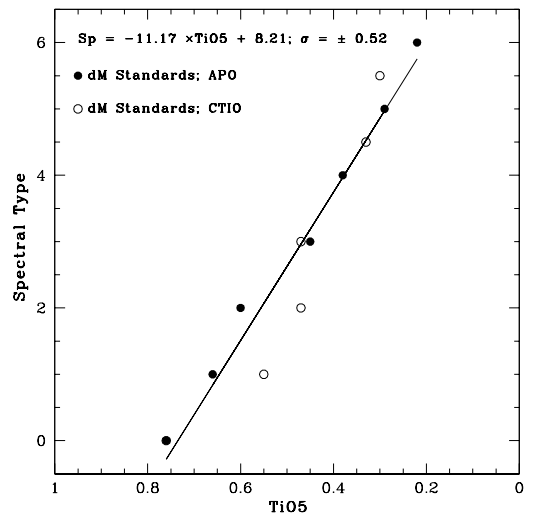


FIG. 1.— The measured TiO5 bandhead strength versus catalog spectral type (Reid, Hawley, & Gizis 1995). The straight line denoted by the equation on the plot is the adopted relation for our sample over the range dM0 $\leq$ Sp $\leq$ dM6. The filled circles are standards observed at APO with $\sim$ 2 Å/pixel resolution and uncertainty of $\pm$ 0.5 spectral type. The open circles are from the lower resolution spectra observed at CTIO with $\sim$ 4 Å/pixel resolution and indicate an uncertainty of $\pm$ 1.0 spectral type.

Calcium Hydride (CaH) features were also measured, as the relative strength of CaH compared to TiO serves to identify subdwarfs as described in Reid & Gizis (1998). We found only one possible subdwarf in the sample, LP164-52.

The equivalent width (EW) of the H$\alpha$ emission line, which is formed in the magnetically heated chromosphere and is commonly used to characterize the magnetic activity of M dwarfs, was measured following the prescription in Hawley, Gizis, & Reid (1996). The H$\alpha$ EW may change dramatically through the M dwarf sequence solely because of the rapidly changing continuum flux in this wavelength region, and not because of a change in the magnetic heating of the chromosphere. However, all of our analysis is carried out on subsamples of objects with the same spectral type, so comparing relative equivalent widths within these subsamples gives a reasonable measure of differences in magnetic activity.

Table 3 gives the measured H$\alpha$ EW and uncertainties

hydride and TiO flux ratios are listed in columns 7-14 followed by the new spectral types as determined from the TiO5 bandheads (column 15). A reference column (16) indicates the designations (dMe, dM(e), or dM) for each M dwarf as discussed further in §4.1. The H$\alpha$ EW and TiO5 ratios are displayed in Figure 2.
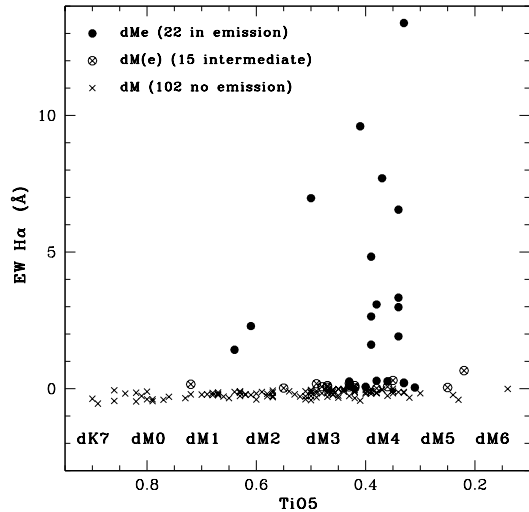


FIG. 2.— The EW in Å of the H$\alpha$ feature for 139 dMs in CPMBs versus the ratio of the flux in the TiO5 molecular band. Filled circles are dMe stars. Open circles with crosses are dM(e) stars and crosses are inactive dM stars.

## 3. DETERMINATION OF WHITE DWARF AGES

We use the photometry of the WDs provided by Smith (1997) for our age determinations. This method introduces somewhat larger uncertainties in age than matching model H line profiles to high S/N data (e.g. Silvestri et al. 2001) but it is accurate enough for our purposes (see Oswalt et al. 1996; Smith 1997, for a discussion of this procedure). The cooling ages were extracted from the model grids as described in Bergeron, Saumon, & Wesemael (1995) using the $V - I$ and $B - V$ colors of the WDs.

The mass of the WD plays the dominant role in determining the WD cooling rate. Hence, it is not surprising that a large uncertainty in the final age from the WD models is associated with the mass estimate. Unfortunately, determining the mass of a WD is not a simple task, and achieving a high precision is even more daunting. At present, there are less than 300 individual WDs for which a mass has been determined and of those, less than 100 have been determined within $\sim 10\%$ precision ($\sigma < 0.05\ M_\odot$).

Silvestri et al. (2001) determined the masses for 44 WDs in the Luyten sample based on the gravitational redshift of the WD. These masses on average have $\sigma_{M_{\rm WD}} > 0.05\ M_\odot$. Silvestri et al. (2001) sampled a significant fraction of the WDs in our current sample. We use their mean mass of $0.61 \pm 0.16\ M_\odot$ as a representative mass of the WDs in our sample. Only three of the WDs in this study have independently measured masses and active (dMe) M dwarf companions (L170-14B, LP617-35, and LP798-13) and when these masses are used in the determination of the ages for these three systems, the ages

ages determined from the mean mass. For consistency, we use the mean mass estimate for all of the WDs in this study. It appears to be a reasonable mean mass assumption since it is close to the mean mass of nearly every WD mass distribution in the literature (see for example Koester 1987; Bergeron, Saumon, & Wesemael 1995; Reid 1996).

Having established an average mass and uncertainty for the WDs in our sample, we next determined the gravities corresponding to our mean mass and error using the mass−radius relation implicit in the WD model calculations. For either the hydrogen- or helium-dominated model atmospheres, the average difference in cooling ages are less than 0.5 Gyr, approximately half the size of the errors imposed by assuming a mean mass for the WD. Adding errors from the photometry and from the mass estimate in quadrature yields the uncertainty in the cooling ages of the WDs for the pure H and He (DA and DB WDs, respectively) atmospheric model results. The average cooling age for our sample is $t_{\rm cool} = 3.06^{+0.94}_{-1.09}$ Gyr for a 0.61 $M_\odot$ mass WD.

### 3.1. Initial→Final Mass Relation for White Dwarfs

The ages and uncertainties calculated above represent the total cooling age of each individual WD (total time after emerging from the planetary nebula). This however, is not the total age of the WD. We need a way of estimating the length of time a 0.61 $M_\odot$ WD exists on the main sequence before evolving to become a WD. The pre-WD lifetime is dependent on the initial mass of the progenitor star. Therefore, it is necessary to determine the main sequence mass of the progenitor star based on the final WD mass. This process is complicated because the progenitor may lose a significant amount of mass during its evolution.

Weidemann (2000) discusses the many factors which determine the final mass of the WD such as rotation, binarity, magnetic fields, mergers, and differential mass loss. The average main sequence mass for a 0.61 $M_\odot$ WD from Weidemann (2000) is $2.17 \pm 0.19\ M_\odot$. Using the third-order polynomial of Iben & Laughlin (1989)

$$\log t_{\rm evol} = 9.921 - 3.6648(\log M_{\rm I}) + 1.9697(\log M_{\rm I})^2 - 0.9369(\log M_{\rm I})^3 \quad (4)$$

we determine the main sequence lifetime corresponding to a given initial mass, where $t_{\rm evol}$ is the main sequence lifetime (in years) of the star and $M_{\rm I}$ is the progenitor mass of the WD (in $M_\odot$).

For our $M_{\rm WD} = 0.61\ M_\odot$ WD mass, this translates into a main sequence lifetime of $0.75^{+0.21}_{-0.15}$ Gyr. We added this value to the individual cooling ages of the WDs ($t_{\rm cool}$) as determined in the previous section. This yields an average age for the WDs in our sample of $3.81^{+0.98}_{-1.09}$ Gyr, near the age of the oldest cluster (M67) in the previous activity−age relations determined by HRT.

## 4. AGE-ACTIVITY RESULTS

### 4.1. H$\alpha$ Emission

In §2.3 we discussed how the EW of the H$\alpha$ emission feature in M dwarfs is used as the primary marker of an active star. For comparison with recent EW studies, we define a feature with positive EW as being in emission and negative EW as being in absorption. Previous studies such as

(1996); Hawley, Reid, & Tourtellot (2000); Gizis, Reid, & Hawley (2002) use a cutoff of 1.0 Å as the minimum EW at which one can unambiguously detect emission in a M dwarf. We measured 23 stars with $0.0 < EW < 1.0$ Å and 14 stars with $EW > 1.0$ Å. Of the 23 low-emission objects, emission was confirmed by eye for only eight stars. In the remaining 15 low-emission stars, the Hα feature is too small to distinguish from the noise. We have decided to include only the eight stars where Hα can be confirmed by eye in our group of M stars with emission (dMe). Though this is a subjective way of establishing a minimum limit of detectability, it ensures that we follow only stars that are definitely in emission through our analysis. In Figure 2, the 22 dMe stars are plotted as filled circles. The 15 stars with questionable emission are plotted as open circles with crosses. We refer to these as dM(e) or intermediate dM stars, and keep track of their location throughout our analysis, in an attempt to deduce their true nature and assess the reliability of detecting emission in M dwarfs with $EW < 1.0$ Å. Finally the stars that were identified as having no Hα emission (dM) are plotted as crosses. We maintain this notation in all subsequent plots. Although some of the dMs may be dM(e) within our uncertainty, we are confident that none of the dM or dM(e) are dMe.

Figure 3 illustrates the fraction of stars in emission per half-spectral class in our sample (solid line) as compared to Hawley, Gizis, & Reid (1996, hereafter HGR - dashed line). Though the number of stars per bin is significantly less for our sample than for HGR the trend toward a higher fraction of dMe to dM stars per 0.5 spectral type is similar (and within the uncertainty) up to a spectral type of ∼ M4.5 where the number of stars in our sample drops precipitously. Only a small fraction of stars are in emission at early M spectral types in both samples.

In Figure 4 we divide the sample by spectral type into seven separate panels. The symbols are the same as given in Figure 2. The top panel contains the earliest spectral type (late K; previously classified as early M dwarfs based on low-resolution spectra) stars in the sample. The next five boxes are spectral types M0, M1, M2, M3, and M4 respectively. The last box contains all of the later type M dwarfs in our sample. The Hα EWs of the stars are plotted (in Å) versus the ages (in Gyr).
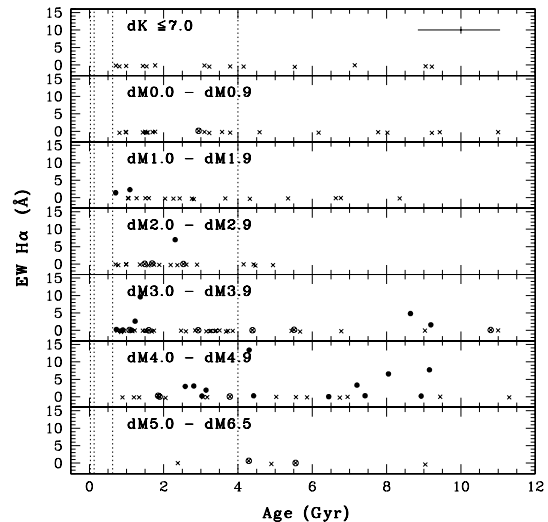


FIG. 4.— The EW Hα per 1.0 spectral type bin versus age for our sample. The filled circles represent the 22 dMe in our sample. The open circles with crosses represent the 15 intermediate dM(e) stars and finally the crosses, all at or below zero EW, are the remaining 102 inactive dMs. Vertical dotted lines indicate the ages derived for clusters observed in the PMSU study. Average error bars are given at the right hand side of the top panel. See text for detailed discussion.

The average error in age (largely a result of the errors in photometry and mass) is approximately ± 1.0 Gyr as shown at the right of the top panel. The actual average errors for the EWs are much smaller (formally $\sigma_{H\alpha} = {}^{+0.03}_{-0.02}$ Å) and arise primarily from the placement of the pseudo-continuum points. The four vertical dotted lines represent the ages of the clusters used in the HRT activity−age relation. The youngest clusters, IC2602 and IC2391, are both ∼ 30 Myr old, while the slightly older clusters NGC2516 and the Pleiades are grouped together at 125 Myr. The third line at 625 Myr is the age of the Hyades cluster and the final line at 4 Gyr is at the age of M67, the oldest cluster in their sample.

There are several important features that warrant discussion in this Figure. First, and not surprisingly, it appears that at early ages (< 4 Gyr), there are active M dwarfs in nearly every well-populated spectral type bin with the exception of M0. A large fraction of our dM(e) stars are located within this age range as well. HRT found that nearly every star in their youngest clusters was active above a certain threshold so it is not surprising that a large fraction of our active stars are apparently young.

However, the majority of our sample is quite old in comparison to the clusters studied by HRT. We have no stars as young as their four youngest clusters and have very few M dwarf stars that are even as young as



FIG. 3.— Ratio of dMe stars to the total number of M stars in each 0.5 spectral class bin. The solid line represents our sample, the dashed line indicates the HGR sample. There are 139 total stars in our sample and 2010 total stars in the HGR sample. As discussed in the text, our sample have very few stars later than type M4.5.

### 4.2. Activity and Age

activity−age relation is well sampled; as expected, our sample will contribute important information on activity at relatively old ages. A large fraction of our stars are older than the oldest cluster (M67 at 4 Gyr) available for the cluster activity−age relation.

Another interesting aspect of Figure 4 is the striking lack of active stars with ages greater than 4 Gyr and spectral types earlier than M3. There are virtually no active M stars earlier than type M3 that are older than roughly 2 Gyr. Stars in our sample with spectral types M3 and later appear to remain active for much longer. Again this agrees qualitatively with the cluster results.

The next three figures (Figures 5-7) show $M_V$, $V − I$, and mass versus log(age) respectively. Table 4 lists the $V − I$, $M_V$, and mass values (columns 4-6) for the active (dMe and dM(e)) stars in Figures 5-7. The $V − I$ colors for the M dwarfs in our sample are from Smith (1997). We determined the $M_V$ for the stars in our sample based on Reid & Hawley (1999) 4$^{\text{th}}$ order polynomial fit relating the $M_V$ to the $V − I$ color of the star as

$$M_V = 3.98 + 1.437(V−I) + 1.073(V−I)^2 − 0.192(V−I)^3. \tag{5}$$

This polynomial proves to be a good fit, in particular to stars with $0.85 < (V − I) < 2.85$. There is an abrupt discontinuity in the slope of $M_V$ versus $V − I$ for dM stars at a $V − I \sim 2.9$ (dM4). Stars at this point have magnitudes $\pm$ 1.5 in $M_V$ in either direction with the midpoint at $M_V \sim 13$. For stars with $V − I \sim 2.9$ in our sample, we assigned the midpoint value of $M_V \sim 13$ with errors of $\pm$ 1.5. For all other stars in Figures 5-7 the uncertainties in $M_V$, $V − I$, and mass are the size of the data points. For clarity, the uncertainties in age are given for only the active stars. The average age uncertainty for the rest of the points is $\pm$ 1 Gy.
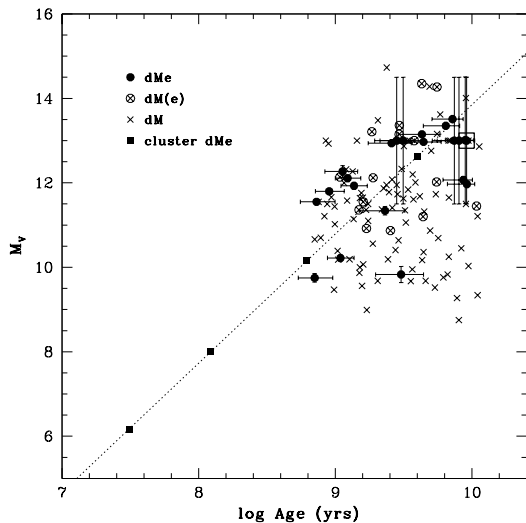


Fig. 5.— The $M_V$ versus log(age) relation for our sample. The points are the same as in previous figures with the addition of the four solid squares representing the cluster ages from the PMSU study along with the corresponding empirical fit (dotted line). The open square denotes the location of LP133−373/374.

The M dwarf masses were determined using the relation from Delfosse et al. (2000):

$$\log \frac{M}{M_\odot} = 10^{-3}[0.3 + 1.87(M_V) +$$
$$7.6140(M_V)^2 − 1.6980(M_V)^3 + 0.060958(M_V)^4], M_V \in$$
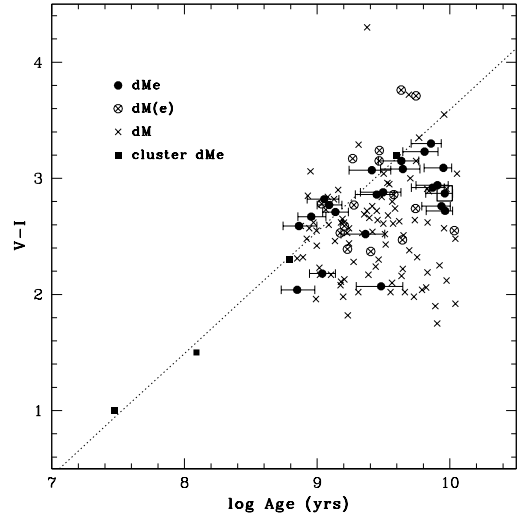


Fig. 6.— The $V − I$ versus log(age) relation for our sample. Symbols are the same as in Figure 5. The open square denotes the location of LP133−373/374.
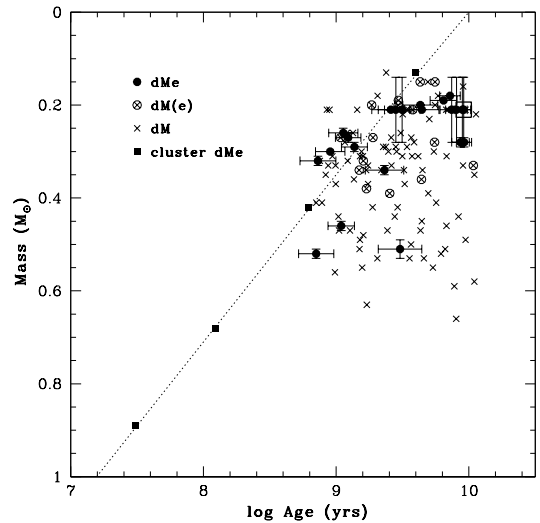


Fig. 7.— The M dwarf mass versus log(age) relation for our sample. Symbols are the same as in Figures 5 and 6. The open square denotes the location of LP133−373/374.

$$(6)$$

Figures 5-7 are directly comparable to the cluster results shown in HRT, and to Figure 11 ($V − I$ plot only) in Gizis, Reid, & Hawley (2002). We reproduce the cluster results on our plots with the dotted line connecting the four filled squares (representing the 4 unique Hα turn-off ages of the six clusters). The cluster age-activity relation identifies the dotted line as the suggested activity limit: stars that are fainter in absolute magnitude, redder in color, and lower in mass at a given age than the value of the relation (i.e. above the line in our plots) should be active, while stars below the line should be inactive. Results for our CPMB systems are shown with the same symbols as in previous plots.

Many of the dMe stars in our sample are more active than the cluster relation would predict. The same is

number of the dMe stars fall below the relation, indicating that with the larger age spread and the sampling of individual variations possible using our CPMB sample, the cluster relation is to simplistic. At the oldest ages we sample, near 10 Gyrs, the dMe stars are often bluer, more massive and, to a lesser extent, brighter than the cluster relation would predict. In other words, magnetic activity is lasting longer in these higher mass stars than is observed in clusters. The average errors in $M_V$ ($< 0.5$ magnitudes), $V - I$ ($< 0.1$ magnitudes), and mass ($< 0.1$ $M_\odot$) cannot account for all of the discrepancy.

We note that one possible source of bias in our sample is the presence of a close, unresolved binary companion. In early M dwarfs, the induced synchronous (fast) rotation of such a system can increase the dynamo heating and produce strong emission even in old systems. Gizis, Reid, & Hawley (2002) point to a few M dwarfs in the D region of their Figure 5 as being active due to the presence of spectroscopically identified binary companions. Fischer & Marcy (1992) show that among binaries with M dwarf components, the incidence of detectable unresolved tertiary components is about 7%. Smith (1997) detected evidence of unresolved tertiary components (via anomalies in $BVRI$ colors) in about 10% of the 500 Luyten-Giclas pairs. Given that binaries comprise about 0.5-0.75 of the stars in the solar neighborhood (Abt 1988), one would expect a sample of single stars to be several times more seriously impacted by unresolved binary pairs than a wide binary sample is impacted by unresolved tertiary components.

To investigate this effect, Oswalt et al. (2004) report on time series photometric observations of all of our pairs which contain active M dwarf components in order to search for light variations in either the WD or main sequence components. Each pair receives at least a half night of observing time. So far, only one, LP133-373/374 (dM4e+DC, black open square in Figures 5-7) has shown any periodic variability that exceeds 2% in amplitude. The dMe component in this pair exhibits partial eclipses with a period of about 19.5 hours, suggesting that its enhanced activity is at least partially due to tidal interaction between two unresolved nearly identical dMe stars. The lightcurves of LP133-373/374 and other wide pairs will be published elsewhere. Nevertheless, the low incidence of short term photometric variability in the CPMB sample suggests that third components in, general, do not appear to account for most of the scatter seen in Figures 5-7.

An interesting finding, which again differs from the cluster results, is that for our binaries, not all M dwarfs that lie above the limiting relation are in emission (inactive M dwarfs are marked as crosses in the Figures). All (of the observed) cluster M dwarf stars that were redder (fainter, less massive) than the limiting relation had H$\alpha$ in emission. This may indicate that stars in clusters are more uniform in their activity evolution than those in the field at the same age. However, again the possibility of unresolved companions, and/or differences in evolution between M dwarfs in clusters and M dwarfs in binary systems with a white dwarf may be causing unknown effects on the magnetic field generation in the M dwarf. As the driving mechanism behind the magnetic heating of the mid-M dwarfs is not well understood, there is no way of predicting the effect of different kinematical or residual orbital effects on such a mechanism. Evidently

variables other than mass and rotation rate may influence the magnetic activity in such old systems. Also, we emphasize that the binaries are from a field star sample with consequent uncertainties in their individual evolution and properties, which contribute to the more complicated nature of their activity−age relation.

In summary, the general trend of lower mass (redder, fainter) stars remaining active longer than was predicted from the cluster results is confirmed. However, the scatter is larger, the activity is not ubiquitous, and the relation is not linear with log(age) for the ages older than 1 Gyr which we sample with our binaries.

## 5. M DWARF KINEMATICS

In this section we examine the kinematics of active and inactive M dwarfs for the sample of 161 M dwarfs in CPMB systems. The sample includes an additional 45 M dwarfs observed after the original investigation of Silvestri, Oswalt, & Hawley (2002, hereafter SOH). Twenty-two of these stars were excluded from the age-activity analysis in the previous section because we did not have photometry for their white dwarf companions and therefore could not determine their ages. However, they are included here because we do have good M dwarf data to determine their space motions. Table 5 gives the new velocity data for the sample, including the 45 WD+dM systems not presented in SOH. Columns 1-3 list the WD name assigned by Luyten, the R.A. and Decl. (coordinates are for equinox 1950). Columns 4-7 list the proper motion, the direction of proper motion, our measured radial velocity ($v_r$), and uncertainty in radial velocity ($\sigma_{v_r}$). Columns 8-15 give the $UVW$-space motions, their uncertainties, and the full space motion of each system. As with previous tables, a reference column (16) indicates the designation (dMe, dM(e), or dM) for each M dwarf. As in SOH, the space velocities are in a left-handed coordinate system.

The metallicity of the M dwarfs, determined by comparing CaH and TiO band strengths provides additional information on the population membership of the CPMB systems. Figure 8 shows the CaH2 versus TiO5 plot originally calibrated by Gizis (1997) to give a rough metallicity estimate for M dwarfs. Metal poor halo stars would lie below and to the right of the disk sequence represented by the bulk of the points plotted in the Figure. LP164−52 remains the only probable subdwarf in this sample. The rest appear to have solar-like metallicities which suggests that all but one of the 161 binaries are part of the Galactic disk population[6].

Figure 9 shows the $U$- versus $V$-velocity components of the space motion for the 161 binaries with good M dwarf spectra. The symbols are similar to those in previous figures, with dMe stars denoted by filled circles, dM(e) stars by open circles with crosses. The dM stars are now represented by open circles for clarity (they were denoted by crosses in previous Figures). As expected from the metallicity results, the stars are nearly all contained within the velocity contours of the Galactic disk (thin and thick components, including the eclipsing M dwarf, LP133−373 at [+19.0, −9.0]). Except for a few obvious outliers (the potential subdwarf,

---

[6] The two objects in the upper right hand portion of Figure 3 of SOH have since been reobserved with higher quality spectra. The new data indicate better agreement with the rest of the sample in
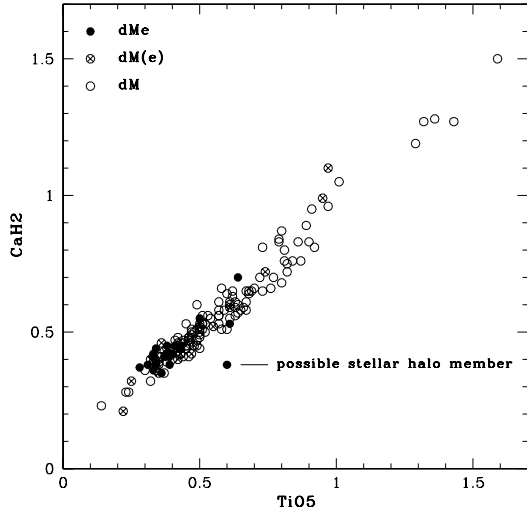
FIG. 8.— The CaH2 versus TiO5 relation for 161 M dwarfs in binary systems. The bandpasses for CaH2 and TiO5 are 6814-6846 Å and 7126-7135 Å, respectively. Symbols are the same as in Figures 5-7 except the dMs are now shown as open circles. We find only one potential subdwarf system, LP164-52.
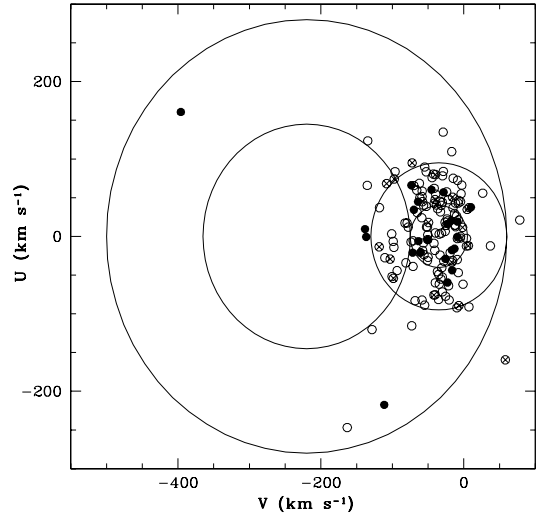
FIG. 9.— The $U$ versus $V$ velocity distribution of 161 binary systems with measured H$\alpha$ EWs and radial velocities. The symbols are the same as in Figure 8. The ellipsoids plot the $1\sigma$ (inner) and $2\sigma$ (outer) contours for the Galactic thick-disk and stellar halo populations, respectively. Typical errors are approximately $\pm$ 10 km s$^{-1}$.

LP164$-$52 at [$-0.7,-136.6$], HZ 43B, LP219$-$78, and LP205$-$28), the active stars have lower average velocities and are more closely confined to the thin disk, in agreement with previous results (Reid, Hawley, & Gizis 1995; Hawley, Gizis, & Reid 1996). The marginally active dM(e) stars, in contrast, are more closely aligned with the higher velocity, inactive dM stars. The plot also reveals a few additional high velocity systems compared to the earlier SOH results. The spectra for these high velocity systems are of equivalent quality to the rest of the spectra and there are no obvious systematic errors which would result in velocities that are larger than the average of the distribution. Their large velocities are likely a result of being part of the high velocity tail of the thin or thick disk population of the Galaxy. The additional data shown in Figure 9 support the conclusions of SOH that the high velocity white dwarf stars in this sample are not part of a dark matter halo, in contrast to the suggestion of Oppenheimer et al. (2001a).

## 6. CONCLUSIONS

We have determined the ages for 139 M dwarf stars in CPMBs to an accuracy of $\pm$ 1 Gyr and have extended the chromospheric activity$-$age relation to ages much older than the oldest open cluster used in previous work. As found in previous work, lower mass (redder, later spectral type) M dwarfs are more likely to be active at old ages than higher mass M dwarfs. However, we have demonstrated that our activity$-$age results for M dwarfs in wide binary systems depart from the log-linear relations seen in cluster M dwarfs. Neither the uncertainties in the age estimates for the binary M dwarfs nor the uncertainties in cluster age estimates can account for the disparity between the two relations. Active M stars of a given age in our sample are found at higher mass, bluer color and brighter absolute magnitude than predicted from the cluster results.

In addition, the activity in our CPMB M dwarfs is not

mass as is found to be the case for M dwarfs in clusters. Evidently the magnetic activity evolution in clusters is more uniform than in these field binaries, at least for ages < 4 Gyr. The same activity behavior we observe may be present in older clusters, which are as yet too faint to be observed. It is not clear what mechanism would selectively allow for emission at a particular age in some old M dwarf stars while prohibiting it in others of the same mass and spectral type at the same age. Possible explanations for the discrepancy include unresolved close companions that induce fast rotation in some M dwarfs even at old ages, or as yet unknown evolutionary effects due to the presence of a companion white dwarf (albeit at a large distance from the M dwarf).

We have successfully extended the activity$-$age relations to ages several Gyr older than the cluster relations, but it is clear that more work needs to be done to increase the number of old M dwarf stars for which accurate ages can be determined. For a more complete picture of old M stars, work must also be done to extend this relation to later spectral types, as our study is not well sampled at types later than M4.5. Recent studies (West et al. 2004) show that magnetic activity is strongly correlated with spectral type in large samples of disk stars, and also depends on distance from the Galactic plane, another age-dependent factor.

In the context of previous work, our analysis suggests that nearly all of our high velocity common proper motion binary WDs are part of a rotating component and have kinematics which resemble the high velocity tail of the Galaxy's disk population as found in SOH. Also, the M dwarf stars in our sample exhibit metallicities indicative of the thick disk component of the Galaxy, just as Reid, Sahu, & Hawley (2001) demonstrated with their large sample of M dwarf stars. Our study of WD+dM systems demonstrates that the active M dwarfs exhibit mostly thin disk kinematics, as expected of a

dwarf companions provide essential confirmation of population membership.

## REFERENCES

Abt, H. A. 1988, Ap&SS, 142, 111

Barry, D. C. 1988, ApJ, 334, 436

Bergeron, P., Ruiz, M.-T., & Leggett, S. 1997, ApJS, 108, 339

Bergeron, P., Saumon, D., & Wesemael, F. 1995, ApJ, 443, 764

Boss, A. P. 1987, ApJ, 319, 141

Boss, A. P. 1988, in Comments on Astrophysics, Vol. 12, 169

Byrne, P. B. 1993a, A&A, 272, 495

Byrne, P. B. & Doyle, J. G. 1990, A&A, 238, 221

Chabrier, G. 1993, ApJ, 414, 695

Dawson, P. C. 1986, ApJ, 311, 984

Delfosse, X., Forveille, T., Ségransan, D., Beuzit, J.-L., Udry, S., Perrier, C., & Mayor, M. 2000, A&A, 364, 217

Ding, M. D. & Fang, C. 2001, MNRAS, 326, 943

Fischer D. A. & Marcy G. W. 1992, ApJ, 396, 178

Giclas, H. L., Burnham, R., & Thomas, N. G. 1971, in Lowell Proper Motion Survey, Northern Hemisphere: The G−Numbered Stars (Flagstaff: Lowell Observatory)

Giclas, H. L., Burnham, R., & Thomas, N. G. 1978, Lowell Observatory Bulletin, 8, 89

Gizis, J. E. 1997, AJ, 113, 806

Gizis, J. E., Reid, I. N., & Hawley, S. L. 2002, AJ, 123, 3356

Hawley, S. L. et al. 2002, AJ, 123, 3409

Hawley, S. L., Gizis, J. E., & Reid, I. N. 1996, AJ, 112, 2799 **HGR**

Hawley, S. L., Reid, I. N., & Tourtellot, J. G. 2000, in La Palma Conf. on Very Low Mass Stars and Brown Dwarfs in Stellar Clusters and Associations, eds. R. Rebolo & M. R. Zapatero-Osorio (Cambridge: Cambridge University Press), 109 **HRT**

Hawley, S. L., Tourtellot, J. G., & Reid, I. N. 1999, AJ, 117, 1341

Hernanz, M., García-Berro, E., Isern, J., Mochkovitch, R., Segretain, L., & Chabrier, G. 1994, ApJ, 434, 652

Iben, I. & Laughlin, G. 1989, ApJ, 341, 312

Isern, J., Hernanz, M., Mochkovitch, R., & García-Berro, E. 1991, A&A, 241, 291

Isern, J., Mochkovitch, R., García-Berro, E., & Hernanz, M. 1997, ApJ, 485, 308

Kirkpatrick, J. D., Henry, T. J., & McCarthy, D. W. 1991, ApJS, 77, 417

Koester, D. 1987, ApJ, 322, 852

La Bonte, A. E. 1970, in IAU Colloq. 7, Proper Motions, ed. W. J. Luyten (Minneapolis: University of Minnesota Minneapolis Press), 26

Lamb, D. Q. & Van Horn, H. M. 1975, ApJ, 200, 306

Liebert, J., Dahn, C. C., & Monet, D. G. 1988, ApJ, 332, 891

Luyten, W. J. 1963, in Proper Motion Survey with the Forty-Eight Inch Telescope (Minneapolis: University of Minnesota Minneapolis Press)

Luyten, W. J. 1969, in Proper Motion Survey with the Forty-Eight Inch Telescope (Minneapolis: University of Minnesota Minneapolis Press)

Luyten, W. J. 1974, in Proper Motion Survey with the Forty-Eight Inch Telescope (Minneapolis: University of Minnesota Minneapolis Press)

Luyten, W. J. 1979, in Proper Motion Survey with the Forty-Eight Inch Telescope (Minneapolis: University of Minnesota Minneapolis Press)

Martín, E. L. & Ardila, D. R. 2001, ApJ, 121, 2758

Mochkovitch, R. 1983, A&A, 122, 212

Noyes, R. W., Hartmann, L. W., Baliunas, S. L., Duncan, D. K., & Vaughan, A. H. 1984, ApJ, 279, 763

O'Neal, D., Neff, J. E., & Saar, S. H. 1998, ApJ, 507, 919

Oppenheimer, B., Hambly, N. C., Digby, A. P., Hodgkin, S. T., & Saumon, D. 2001a, Science, 292, 698

Oswalt, T. D., Hintzen, P. M., & Luyten, W. J. 1988, ApJS, 66, 391

Oswalt, T. D., Rudkin, M. A., Johnston, K., Kissinger, J., & Menezes, K. 2004, in ASP Conf. Proc. of the 14th European Workshop on White Dwarfs, eds. D. Koester & S. Jordan (Dordrecht: Kluwer), in press.

Oswalt, T. D., Sion, E. M., Hintzen, P. M., & Liebert, J. W. 1991, in Proc. of European Workshop 7, White Dwarfs, eds. G. Vauclair & E. M. Sion (ASP), 379

Oswalt, T. D. & Smith, J. A. 1995, in Proc. of the European Workshop 9, White Dwarfs, eds. by D. Koester & K. Werner (Berlin: Springer-Verlag), 24

Oswalt, T. D., Smith, J. A., Shufelt, S., Hintzen, P. M., Leggett, S. K., Liebert, J., & Sion, E. M. 1993, in Proc. of the European Workshop 8, White Dwarfs: Advances in Observation and Theory, ed. M. A. Barstow (Dordrecht: Kluwer), 419

Oswalt, T. D., Smith, J. A., Wood, M. A., & Hintzen, P. 1996, Nature, 382, 692

Pettersen, B. R., Lambert, D. L., Tomkin, J., Sandmann, W. H., & Lin, H. 1987, A&A, 183, 66

Pettersen, B. R. & Hawley, S. L. 1989, A&A, 217, 187

Pringle, J. E. 1989, MNRAS, 239, 361

Reid, I. N. 1996, AJ, 111, 2000

Reid, I. N. & Gizis, J. E. 1998, AJ, 116, 2929

Reid, I. N. & Hawley, S. L. 1999, AJ, 117, 343

Reid, I. N., Hawley, S. L., & Gizis, J. E. 1995, AJ, 110, 1838

Reid, I. N., Hawley, S. L., & Mateo, M. 1995, MNRAS, 272, 828

Reid, I. N., Sahu, K. C., & Hawley, S. L. 2001, ApJ, 559, 942

Salaris, M., García-Berro, E., Hernanz, M., Isern, J., & Saumon, D. 2000, ApJ, 544, 1036

Segretain, L., Chabrier, G., Hernanz, M., García-Berro, E., Isern, J., & Mochkovitch, R. 1994, ApJ, 434, 641

Silvestri, N. M., Oswalt, T. D., Wood, M. A., Smith, J. A., Reid, I. N., & Sion, E. M. 2001, AJ, 121, 503

Silvestri, N. M., Oswalt, T. D., & Hawley, S. L. 2002, AJ, 124, 1118 **SOH**

Skumanich, A. 1972, ApJ, 171, 565

Smith, J. A. 1997, Ph.D. thesis, Florida Institute of Technology

Smith, J. A. & Oswalt, T. D. 1995, in Proc. of the ESO Workshop, The Bottom of the Main Sequence−and Beyond, ed. C. G. Tinney (Berlin: Springer-Verlag), 113

Soderblom, D. R., Duncan, D. K., & Johnson, D. R. H. 1991, ApJ, 375, 722

Stauffer, J. R., Giampapa, M. S., Herbst, W., Vincent, J. M., Hartmann, L. W., & Stern, R. A. 1991, ApJ, 374, 142

Weidemann, V. 2000, A&A, 363, 647

West, A. A., Hawley, S. L., Walkowicz, L. M., Covey, K. R., Silvestri, N. M., Raymond, S. N., Harris, H. C., Munn, J. A., & McGehee, P. 2004, AJ, 128, 426

Wilson, O. C. 1966, ApJ, 144, 695

Wood, M. A. 1990, Ph.D. thesis, The University of Texas at Austin

Wood, M. A. 1992, ApJ, 386, 539

Wood, M. A. & Oswalt, T. D. 1998, ApJ, 497, 870

TABLE 1
Complete M Dwarf−White Dwarf Wide Binary Target List.

| Identifier (Sp.1/Sp.2) | R.A. (B1950) | Decl. (B1950) | $V1$ | Sp.1[a] | $V2$ | Sp.2[a] | Site | U.T. (mm/yy) | Exp. (sec) | $\mu$ ($''$/yr) | $\Theta_\mu$ (deg) | Pos. (deg) | Sep. ($''$) |
|---|---|---|---|---|---|---|---|---|---|---|---|---|---|
| (1) | (2) | (3) | (4) | (5) | (6) | (7) | (8) | (9) | (10) | (11) | (12) | (13) | (14) |
| LP349−14/13 | 00:22:06 | 27:24:00 | 13.40 | dM | 16.86 | DB | APO | 06/01 | 300 | 0.12 | 90 | 305 | 113 |
| G158−77/78 | 00:23:28 | -10:53:30 | 13.47 | sdM1 | 16.23 | DA | APO | 09/00,06/01 | 300 | 0.27 | 160 | 127 | 90 |
| G171−B10A/B | 00:23:53 | 38:52:24 | 15.97 | DA | 15.26 | dM5 | APO | 09/00 | 900 | 0.20 | 132 | 202 | 25 |
| L170−14A/B | 00:27:30 | -54:58:00 | 14.84 | dM3.5 | 16.23 | DA | CTIO | 01/02 | 900 | 0.36 | 240 | 327 | 3 |
| G218−8/7 | 00:38:30 | 55:33:42 | 14.1 | DQ5 | 14.02 | dM | APO | 09/00 | 1000 | 0.32 | 103 | 246 | 11 |
| LP825−712/713 | 00:40:36 | -22:02:00 | 15.7 | sdM1 | 18.0 | DA3 | APO | 09/01 | 900 | 0.50 | 83 | 50 | 23 |
| LP242−11/12 | 00:52:30 | 38:32:00 | 13.80 | dM0 | 18.29 | DC | APO | 09/00,09/01 | 300 | 0.50 | 242 | 56 | 22 |
| LP1−169/170 | 01:01:00 | 86:40:00 | 15.2 | dM1 | 16.7 | DQ | APO | 12/00 | 450 | 0.13 | 73 | 326 | 7 |
| Wolf 53/LP79−8 | 01:02:51 | 61:04:18 | 14.87 | dM5 | 18.22 | DC | APO | 09/00 | 800 | 0.48 | 137 | 302 | 9 |
| LP586−65/64 | 01:04:14 | 01:32:42 | 17.28 | DA | 18.35 | dM5 | APO | 09/01 | 1800 | 0.25 | 89 | 213 | 175 |
| LP587−44/45 | 01:19:15 | -00:26:30 | 16.42 | DB | 18.07 | sdM5 | APO | 09/01 | 2400 | 0.19 | 230 | 264 | 9 |
| LP587−54/53 | 01:20:42 | -02:24:48 | 12.62 | dM2 | 17.48 | DC | APO | 10/00 | 150 | 0.22 | 79 | 199 | 44 |
| LP29−148/149 | 01:23:48 | 73:12:00 | 16.8 | DA | 17.0 | dM5 | APO | 09/01 | 1200 | 0.23 | 290 | 43 | 69 |
| G34−48/49 | 01:42:31 | 23:02:48 | 13.08 | sdM3 | 16.9 | DC4 | APO | 10/00 | 240 | 0.32 | 112 | 60 | 24 |
| LP352−31/30 | 01:45:06 | 21:32:00 | 15.41 | dM5 | 18.32 | DA | APO | 10/00 | 600 | 0.20 | 80 | 270 | 13 |
| G244−37/36 | 01:48:12 | 64:11:24 | 11.39 | dM2 | 13.96 | DA6 | APO | 12/00 | 180 | 0.29 | 129 | 178 | 16 |
| G71−B5A/B | 01:50:31 | 08:56:42 | 14.21 | dM4 | 17.22 | DZ | APO | 10/00 | 800 | 0.10 | 154 | 311 | 13 |
| G272−B2A/B | 01:58:32 | -16:00:36 | 14.71 | DBA | 16.02 | dM3 | APO | 09/01 | 600 | 0.13 | 81 | 164 | 7 |
| LP885−23/22 | 02:04:51 | -30:38:30 | 14.14 | dM5 | 16.92 | DA | CTIO | 01/02 | 160 | 0.25 | 124 | 313 | 73 |
| LP245−17/18 | 02:17:21 | 37:33:48 | 13.8 | dM5 | 18.1 | DA | APO | 12/00 | 180 | 0.35 | 102 | 90 | 2 |
| LP590−143/142 | 02:25:52 | 00:24:30 | 18.08 | DA | 17.85 | dM5 | APO | 10/00 | 1500 | 0.11 | 155 | 316 | 73 |
| LP530−22/21 | 02:28:34 | 07:57:24 | 17.38 | DC | 17.77 | dM5 | APO | 02-09/01 | 2700 | 0.35 | 134 | 158 | 23 |
| LP197−55/56 | 02:46:12 | 43:24:00 | 18.78 | DC | 18.40 | dM4.5e | APO | 10/01 | 2400 | 0.26 | 71 | 69 | 10 |
| LP411−23/22 | 02:52:54 | 20:54:00 | 17.58 | DA | 18.78 | dM4.5 | $\cdots$ | $\cdots$ | $\cdots$ | 0.25 | 118 | 40 | 12 |
| LP355−11/10 | 02:57:42 | 24:42:00 | 16.81 | dM5 | 18.52 | DC | APO | 02/01 | 1800 | 0.18 | 124 | 239 | 138 |
| LP472−39/38 | 03:17:18 | 11:24:00 | 14.55 | dM0 | 19.05 | DQ | APO | 12/00 | 450 | 0.18 | 192 | 23 | 17 |
| LP355−64/65 | 03:19:30 | 26:59:00 | 11.5 | dM1 | 17.6 | DA | APO | 10/00 | 100 | 0.21 | 113 | 98 | 278 |
| LP31−139/140 | 03:24:30 | 73:15:00 | 17.5 | DC7 | 16.48 | dM4.5e | APO | 12/00 | 1500 | 0.43 | 141 | 9 | 12 |
| LP356−87/88 | 03:25:00 | 26:21:00 | 13.62 | dM | 17.66 | DA | APO | 10/00,02/01 | 600 | 0.18 | 120 | 309 | 6 |
| LP888−64/63 | 03:26:45 | -27:18:36 | 13.9 | DA | 15.3 | sdM3 | CTIO | 02/02 | 600 | 0.83 | 63 | 227 | 7 |
| LP773−12/11 | 03:31:48 | -16:05:00 | 15.03 | dM5 | 18.52 | DC | APO | 10/00 | 600 | 0.32 | 80 | 235 | 6 |
| LP31−276/277 | 03:54:36 | 70:47:00 | 12.96 | dM0 | 18.37 | DC | APO | 01/01 | 400 | 0.17 | 74 | 185 | 9 |
| LP889−21/20 | 03:58:06 | -32:06:00 | 15.72 | dM5 | 18.63 | DC | CTIO | 01/02 | 480 | 0.21 | 117 | 276 | 10 |
| 40 Eri−A | 04:13:03 | -07:44:06 | $\cdots$ | dG8 | $\cdots$ | $\cdots$ | $\cdots$ | $\cdots$ | $\cdots$ | 4.08 | 213 | 105 | 82 |
| 40 Eri−C/B | 04:13:03 | -07:44:06 | 4.35 | dM5e | 9.51 | DA4 | $\cdots$ | $\cdots$ | $\cdots$ | 4.08 | 213 | 105 | 82 |
| LP415−1/2 | 04:17:12 | 19:47:00 | 16.33 | dM5 | 17.88 | DA | APO | 01-02/01 | 1600 | 0.17 | 216 | 138 | 30 |
| LP775−52/53 | 04:19:26 | -16:07:06 | 12.56 | dM0 | 17.42 | DA | APO | 10/00 | 200 | 0.35 | 112 | 142 | 12 |
| G175−34A/B | 04:26:50 | 58:53:18 | 11.88 | dM5 | 12.39 | DC5 | APO | 12/00 | 60 | 2.37 | 146 | 82 | 6 |
| HZ 9A/B | 04:29:24 | 17:38:00 | 13.95 | DA2 | 18.0 | dM1 | APO | 01-02/01 | 1800 | 0.12 | 110 | 103 | 13 |
| BD+26°730/LP358−52A | 04:32:54 | 26:56:00 | 18.32 | DA | 18.75 | DC | APO | 12/00 | 2700 | 0.11 | 108 | 118 | 1 |
| LP358−52B | 04:32:54 | 26:56:00 | 18.0 | sdM1 | $\cdots$ | $\cdots$ | APO | 12/00 | 2700 | 0.11 | 108 | 118 | 1 |
| LP891−13/12 | 04:43:18 | -27:32:00 | 15.41 | dM4.5e | 16.69 | DQ | CTIO | 01/02 | 400 | 0.24 | 246 | 62 | 49 |
| G86−B1A/B | 05:18:26 | 33:19:12 | 14.26 | dM5 | 15.98 | DAe | APO | 10/00 | 900 | 0.18 | 113 | 203 | 9 |
| LP120−25/26 | 05:51:48 | 56:02:00 | 18.80 | sdM0 | 18.1 | DA | APO | 01/01 | 1800 | 0.14 | 115 | 300 | 7 |
| LP120−27 | 05:51:48 | 56:02:00 | 14.0 | dK | $\cdots$ | $\cdots$ | APO | 01/01 | 500 | 0.14 | 115 | 300 | 7 |
| LP159−33/32 | 05:51:59 | 46:50:54 | 17.13 | dM5 | 15.47 | DC | APO | 01-02/01 | 1800 | 0.54 | 179 | 219 | 12 |
| LP779−19/20 | 06:04:18 | -19:50:00 | 17.22 | DQ | 18.38 | dM5 | CTIO | 01/02 | 1800 | 0.23 | 108 | 53 | 43 |
| G105−B2A/B | 06:25:01 | 10:02:30 | 13.16 | dM2 | 16.48 | DCZ6 | APO,CTIO | 01/01,01/02 | 400 | 0.10 | 151 | 310 | 127 |
| LP600−42/43 | 06:28:08 | -02:03:42 | 15.36 | DA | 15.56 | dM5 | APO,CTIO | 01/01,01/02 | 800 | 0.25 | 214 | 307 | 4 |
| LP205−27/28 | 06:41:50 | 43:48:36 | 15.53 | DA | 18.41 | dM5 | APO | 01/01 | 2400 | 0.12 | 176 | 107 | 143 |
| G87−29/28 | 07:06:52 | 37:45:24 | 15.60 | DQ8 | 14.60 | dM4.5e | APO | 01/01 | 540 | 0.44 | 222 | 224 | 15 |
| LP422−6/7 | 07:09:18 | 19:24:00 | 17.19 | DA | 16.24 | dM5 | APO | 01/01 | 1200 | 0.10 | 147 | 179 | 284 |
| LP5−74/73 | 07:26:00 | 82:44:00 | 15.08 | dM0 | 18.73 | DC | APO | 01/01 | 500 | 0.18 | 76 | 279 | 5 |

TABLE 1 — *Continued*

| Identifier (Sp.1/Sp.2) | R.A. (B1950) | Decl. (B1950) | V1 | Sp.1[a] | V2 | Sp.2[a] | Site | U.T. (mm/yy) | Exp. (sec) | $\mu$ (''/yr) | $\Theta_\mu$ (deg) | Pos. (deg) | Sep. ('') |
|---|---|---|---|---|---|---|---|---|---|---|---|---|---|
| (1) | (2) | (3) | (4) | (5) | (6) | (7) | (8) | (9) | (10) | (11) | (12) | (13) | (14) |
| LP207−7/8 | 07:26:06 | 39:17:00 | 15.81 | DA | 15.12 | dM5 | APO | 12/00 | 900 | 0.12 | 186 | 50 | 44 |
| G107−69/70 | 07:27:02 | 48:19:06 | 13.52 | sdM5 | 14.65 | DC9 | APO | 01/01 | 400 | 1.34 | 191 | 155 | 105 |
| LP783−3/2 | 07:38:02 | -17:17:24 | 13.05 | DZQ6 | 16.67 | dM | APO | 01/01 | 1200 | 1.26 | 117 | 276 | 21 |
| LP366−2/3 | 07:41:37 | 24:50:24 | 15.29 | dM5 | 16.52 | DA | APO | 01-04/01 | 1200 | 0.10 | 260 | 86 | 101 |
| LP208−33/32 | 08:04:18 | 44:40:00 | 15.40 | dM5 | 17.77 | DA | APO | 01/01 | 600 | 0.10 | 200 | 280 | 18 |
| LP664−16/15 | 08:06:30 | -04:23:00 | 12.98 | dM2 | 18.26 | DC | APO | 01/01 | 300 | 0.12 | 182 | 220 | 20 |
| LP163−120/121 | 08:07:24 | 48:25:00 | 15.61 | dM2 | 18.10 | DA8 | APO | 01/01 | 800 | 0.14 | 79 | 40 | 11 |
| G111−72/71 | 08:16:47 | 38:44:18 | 13.12 | sdM2 | 16.55 | DAZ7 | APO | 01/01 | 400 | 0.38 | 212 | 258 | 34 |
| L186−119/120 | 08:20:42 | -58:32:00 | 16.58 | DA | 15.85 | dM5 | CTIO | 01/02 | $\cdots$ | 0.20 | 289 | 85 | 21 |
| LP164−52/51 | 08:42:48 | 49:37:00 | 18.31 | DA | 19.30 | dM0 | APO | 01/01 | 2400 | 0.31 | 159 | 296 | 5 |
| LP844−26/25 | 08:51:42 | -24:36:00 | 18.07 | DC | 18.03 | dM4.5e | APO | 01/01 | 2400 | 0.64 | 78 | 270 | 18 |
| LP60−359A/B | 08:52:24 | 63:03:00 | 15.31 | DA9 | 16.94 | dM5e | APO | 12/00 | 2700 | 0.11 | 110 | 65 | 36 |
| LP90−70/71 | 08:55:40 | 60:28:18 | 16.34 | DBQ | 15.68 | dM | APO | 01/01 | 800 | 0.53 | 216 | 60 | 44 |
| LP845−9/8 | 08:58:42 | -22:02:00 | 14.68 | dM2 | 18.37 | DC | APO | 01/01 | 540 | 0.19 | 319 | 288 | 5 |
| LP60−177/178 | 08:59:30 | 68:17:00 | 15.14 | dM1 | 18.71 | DA | APO | 01-02/01 | 2700 | 0.16 | 215 | 3 | 12 |
| LP313−12/13 | 09:04:30 | 27:49:00 | 17.97 | DA | 17.47 | dM4.5e | APO | 01/01 | 1800 | 0.13 | 160 | 36 | 24 |
| LP313−16/15 | 09:06:18 | 29:42:00 | 15.74 | DA3 | 15.61 | dM5 | APO | 01/01 | 800 | 0.14 | 237 | 324 | 11 |
| LP36−141/142 | 09:06:48 | 72:45:00 | 18.59 | DZ | 19.31 | dM5 | $\cdots$ | $\cdots$ | $\cdots$ | 0.12 | 195 | 143 | 11 |
| LP369−15/14 | 09:08:51 | 22:40:06 | 18.28 | DA | 19.32 | dM1 | $\cdots$ | $\cdots$ | $\cdots$ | 0.11 | 120 | 277 | 200 |
| LP60−237/236 | 09:11:24 | 65:09:00 | 13.61 | dM1 | 17.32 | DC | APO | 01/01 | 300 | 0.14 | 241 | 310 | 6 |
| LP487−25/26 | 09:16:00 | 11:11:00 | 18.38 | DC | 17.37 | dM4.5e | APO | 01/01 | 1800 | 0.35 | 235 | 77 | 25 |
| LP787−26/25 | 09:18:30 | -17:16:00 | 17.78 | DA | 17.84 | dM4.5e | APO,CTIO | 01/01,02 | 2400 | 0.20 | 323 | 253 | 13 |
| G117−B15A/B | 09:21:13 | 35:29:48 | 15.45 | DAV4 | 15.99 | dM2 | APO | 01/01 | 1200 | 0.14 | 264 | 126 | 15 |
| G161−36/37 | 09:26:51 | -03:57:00 | 14.76 | DA | 15.21 | dM5 | APO | 01/01 | 600 | 0.27 | 274 | 180 | 19 |
| LP668−10/9 | 09:37:24 | -09:32:00 | 15.86 | dM4.5e | 17.25 | DC | APO | 01-02/01 | 1800 | 0.25 | 157 | 353 | 13 |
| LP488−20/19 | 09:37:42 | 09:21:00 | 16.82 | dM | 18.09 | DC9 | APO,CTIO | 01/01,02 | 1800 | 0.26 | 255 | 241 | 9 |
| LP370−41/40 | 09:41:00 | 22:34:00 | 17.14 | DA | 17.82 | dM | APO | 04/01 | 1800 | 0.12 | 201 | 190 | 13 |
| G117−B11A/B | 09:43:23 | 33:05:18 | 15.10 | dM5 | 17.12 | DA | APO | 01/01 | 500 | 0.14 | 133 | 11 | 14 |
| LP62−34A/35 | 10:04:36 | 66:34:00 | 12.29 | dM | 14.67 | DZ | APO | 01/01 | 900 | 0.21 | 224 | 312 | 56 |
| LP62−34B | 10:04:36 | 66:34:00 | 16.0 | DC | $\cdots$ | $\cdots$ | APO | 01/01 | 900 | 0.21 | 224 | 180 | 3 |
| LP847−41/40 | 10:10:18 | -23:58:00 | 16.90 | dM5 | 18.29 | DAZ | CTIO | 01/02 | 700 | 0.18 | 312 | 315 | 17 |
| CD−18°3019/LP791−55 | 10:43:30 | -18:50:00 | 11.04 | dM0e | 15.49 | DQ9 | APO | 01/01 | 120 | 1.98 | 250 | 356 | 7 |
| LP214−11/10 | 10:54:24 | 41:59:00 | 13.02 | dM1.5 | 18.62 | DC | APO | 12/00 | 1800 | 0.13 | 210 | 318 | 189 |
| LP317−25/26 | 10:54:24 | 30:30:00 | 14.98 | dM0 | 17.89 | DC | APO | 01/01 | 500 | 0.16 | 270 | 8 | 158 |
| LP731−37A/B | 10:59:06 | -11:57:00 | 18.3 | WD | 17.5 | dM5 | CTIO | 02/02 | 1800 | 0.40 | 254 | 229 | 2 |
| LP551−66/67 | 11:04:30 | 04:25:00 | 15.4 | DA | 17.7 | sdM5 | APO | 02/01 | 2400 | 0.19 | 177 | 188 | 3 |
| LP214−39/38 | 11:05:12 | 41:16:00 | 11.86 | dM1 | 16.25 | DC | APO | 01/01 | 200 | 0.21 | 275 | 197 | 11 |
| LP672−1/2 | 11:05:30 | -04:53:00 | 13.10 | DA3 | 12.60 | dM6 | APO | 01/01 | 220 | 0.44 | 184 | 160 | 279 |
| CD−25°8487/LP849−5 | 11:07:00 | -25:43:00 | 8.66 | sdM0 | 17.64 | DC | CTIO | 01/02 | 2 | 0.25 | 106 | 181 | 100 |
| LP373−85/84 | 11:08:48 | 25:35:00 | 17.16 | dM | 19.05 | DCZ | APO | 02/01 | 1800 | 0.24 | 266 | 309 | 72 |
| LP792−6/5 | 11:11:30 | -18:47:00 | 15.73 | dM5 | 18.33 | DC | APO | 02/01 | 1200 | 0.25 | 300 | 215 | 26 |
| LP552−48/49 | 11:20:54 | 07:18:00 | 10.35 | dM1 | 17.49 | DC | APO | 02/01 | 120 | 0.20 | 110 | 113 | 24 |
| LP906−23/24 | 11:20:54 | -32:07:00 | 16.46 | dM5 | 18.44 | DA7 | CTIO | 01/02 | 600 | 0.24 | 282 | 121 | 19 |
| LP906−34/33 | 11:32:54 | -29:53:00 | 14.45 | dM5 | 15.50 | dM5 | CTIO | 01/02 | 400 | 0.16 | 227 | 347 | 4 |
| LP906−35A/B | 11:32:54 | -29:53:00 | 17.41 | DA7 | 17.8 | dM | CTIO | 01/02 | 1800 | 0.16 | 227 | 188 | 52 |
| LP493−16/15 | 11:33:48 | 08:19:00 | 13.84 | dM | 17.37 | DZ | APO | 02/01 | 500 | 0.25 | 245 | 210 | 6 |
| G148−7/6 | 11:43:21 | 32:06:12 | 13.73 | DA3.5 | 14.05 | dM5 | APO | 01/01 | 300 | 0.28 | 203 | 271 | 9 |
| LP375−51/50 | 11:47:46 | 25:35:18 | 15.66 | DA5 | 15.50 | dM2 | APO | 02/01 | 1500 | 0.30 | 252 | 252 | 36 |
| LP493−61/60 | 11:48:48 | 13:11:00 | 14.16 | dM | 19.01 | DC | APO | 02/01 | 500 | 0.21 | 182 | 252 | 44 |
| LP129−587/586 | 11:48:48 | 54:28:00 | 16.65 | DA5 | 16.41 | dM5 | APO | 02/01 | 1200 | 0.25 | 264 | 182 | 35 |
| LP673−42A/B | 11:50:43 | -07:05:36 | 11.96 | dM2 | 19.0 | DC | APO | 02/01 | 300 | 0.54 | 198 | 110 | 9 |
| ESO440−55A/B | 12:04:03 | -31:20:30 | 19.12 | DZ7 | 19.91 | dM5 | CTIO | 01/02 | $\cdots$ | 0.22 | 273 | $\cdots$ | 5 |
| LP674−29/CD−5°3450 | 12:09:48 | -06:05:00 | $\cdots$ | $\cdots$ | $\cdots$ | $\cdots$ | CTIO | 01/02 | 1800 | 0.44 | 220 | 102 | 202 |
| LP216−75/74 | 12:11:06 | 39:18:00 | 16.0 | dM0 | 16.5 | DA | APO | 02/01 | 1200 | 0.13 | 302 | 250 | 15 |

TABLE 1 — *Continued*

| Identifier (Sp.1/Sp.2) (1) | R.A. (B1950) (2) | Decl. (B1950) (3) | V1 (4) | Sp.1[a] (5) | V2 (6) | Sp.2[a] (7) | Site (8) | U.T. (mm/yy) (9) | Exp. (sec) (10) | $\mu$ (''/yr) (11) | $\Theta_\mu$ (deg) (12) | Pos. (deg) (13) | Sep. ('') (14) |
|---|---|---|---|---|---|---|---|---|---|---|---|---|---|
| LP554−64/65 | 12:14:18 | 03:14:00 | 13.28 | sdM3 | 14.9 | DA | APO | 01/01 | 300 | 0.70 | 293 | 190 | 2 |
| LP320−644/643 | 12:15:06 | 32:22:00 | 15.01 | dM | 16.99 | DC7 | APO | 02/01 | 900 | 0.26 | 234 | 330 | 6 |
| LP435−58/59 | 12:20:24 | 19:06:00 | 17.26 | DA | 16.79 | dM | APO | 02-03/01 | 1800 | 0.19 | 268 | 90 | 22 |
| LP795−13/14 | 12:22:48 | -16:50:00 | 18.19 | DA | 17.18 | dM5 | APO | 01/01 | 1800 | 0.12 | 211 | 137 | 28 |
| LP495−176/177 | 12:30:36 | 12:16:00 | 16.52 | dM | 19.24 | DC | APO | 02/01 | 1500 | 0.16 | 284 | 165 | 8 |
| LP321−206/205 | 12:30:42 | 26:22:00 | 19.39 | DC | 18.63 | dM | APO,CTIO | 04/01,01/02 | 3000 | 0.15 | 263 | 3 | 38 |
| LP321−396/397 | 12:38:20 | 28:13:48 | 17.40 | DA | 19.19 | dM4.5e | $\cdots$ | $\cdots$ | $\cdots$ | 0.13 | 259 | 173 | 7 |
| LP20−406/407 | 12:40:30 | 75:26:00 | 16.2 | DA4 | 17.6 | dM | APO | 03/01 | 1800 | 0.23 | 266 | 129 | 6 |
| LP321−458/459 | 12:43:34 | 30:19:54 | 18.5 | DAB | 19.5 | dM | $\cdots$ | $\cdots$ | $\cdots$ | 0.12 | 173 | 90 | 2 |
| G61−16/17 | 12:44:44 | 14:58:24 | 13.51 | sdM2 | 15.82 | DA5 | APO | 01-04/01 | 300 | 0.43 | 298 | 47 | 25 |
| LP497−29/30 | 13:11:30 | 11:14:00 | 17.42 | dM4 | 18.64 | DA | APO | 04-06/01 | 1800 | 0.24 | 207 | 187 | 37 |
| LP910-16/17 | 13:04:42 | -27:47:00 | $\cdots$ | dM | $\cdots$ | WD | CTIO | 01/02 | 1200 | 0.10 | 54 | 231 | 115 |
| HZ 43A/B | 13:14:00 | 29:22:00 | 12.68 | DA1 | 13.0 | dM | APO,CTIO | 01/01,01/02 | 300 | 0.16 | 240 | 280 | 3 |
| LP617−34/35 | 13:17:42 | -02:08:00 | 15.11 | dM5 | 18.84 | DC | APO | 01-04/01 | 900 | 0.19 | 159 | 103 | 23 |
| G14−58/57 | 13:27:40 | -08:18:48 | 12.33 | DA4 | 14.32 | dM5e | APO | 01/01 | 400 | 1.24 | 247 | 160 | 504 |
| LP21−153/152 | 13:30:00 | 79:20:00 | 16.7 | dM0 | 17.0 | DA | APO | 02/01 | 2700 | 0.10 | 290 | 265 | 4 |
| LP798−13/14 | 13:34:18 | -16:04:00 | 15.33 | DA3 | 13.76 | dM5e | APO | 01/01 | 400 | 0.12 | 246 | 242 | 14 |
| LP738−42/43 | 13:34:48 | -11:48:00 | 14.93 | dM5 | 18.10 | DC | APO | 02/01 | 1200 | 0.19 | 199 | 19 | 18 |
| LP498−26/25 | 13:36:45 | 12:23:48 | 14.72 | DB3 | 14.02 | dM4 | APO | 02/01 | 400 | 0.19 | 134 | 307 | 87 |
| LP380−6/5 | 13:45:44 | 23:50:00 | 15.64 | DC9 | 15.41 | dM4 | APO | 04/01 | 900 | 1.48 | 276 | 231 | 188 |
| LP219−77/78 | 13:48:18 | 41:48:00 | 17.20 | DA | 17.59 | dM5 | APO | 04/01 | 2400 | 0.14 | 160 | 98 | 8 |
| LP856−54/53 | 13:48:30 | -27:19:00 | 12.59 | dM3 | 15.20 | DA6 | APO | 02/01 | 600 | 0.24 | 199 | 233 | 9 |
| LP439−180/179 | 14:00:42 | 16:04:00 | 17.38 | dM0 | 18.33 | DA | APO | 04/01 | 1800 | 0.08 | 167 | 238 | 31 |
| LP133−373/374 | 14:02:24 | 50:36:00 | 15.31 | dM5e | 18.42 | DC | APO | 02/01 | 1200 | 0.20 | 308 | 122 | 5 |
| LP799−73/74 | 14:09:36 | -18:29:00 | 17.12 | DC | 16.41 | dM4.5 | APO | 03/01 | 1200 | 0.19 | 133 | 119 | 52 |
| LP66−587/586 | 14:16:06 | 63:18:00 | 15.86 | dM0e | 17.49 | DA | APO | 02/01 | 1500 | 0.09 | 140 | 356 | 8 |
| G200−40/39 | 14:25:59 | 54:01:00 | 11.92 | sdM | 15.06 | DBA4 | APO | 02/01 | 400 | 0.39 | 294 | 349 | 39 |
| LP621−35/36 | 14:50:00 | -00:39:00 | $\cdots$ | dM | $\cdots$ | WD | CTIO | 01/02 | 1800 | 0.19 | 147 | 7 | 9 |
| LP135−154/155 | 15:10:34 | 56:36:12 | 16.33 | DA6 | 15.85 | dM | APO | 02/01 | 1500 | 0.38 | 217 | 86 | 18 |
| LP223−13/14 | 15:25:30 | 43:23:30 | 16.47 | DA | 18.40 | dM5 | APO | 03/01 | 2400 | 0.14 | 186 | 119 | 64 |
| LP176−59/60 | 15:33:12 | 46:59:00 | 17.57 | dM5 | 18.23 | DC9 | APO | 03/01 | 1800 | 0.51 | 296 | 71 | 85 |
| LP743−24/25 | 15:39:12 | -13:47:00 | 18.74 | DC | 17.81 | dM3 | APO | 03/01 | 2400 | 0.20 | 314 | 218 | 7 |
| L480−84/85 | 15:41:54 | -38:10:00 | 14.00 | dM3 | 15.23 | DA | CTIO | 01/02 | 120 | 0.09 | 162 | 261 | 10 |
| LP916−27/26 | 15:42:18 | -27:30:00 | 15.38 | DB4 | 15.18 | dM5 | APO | 06/01 | 900 | 0.24 | 235 | 330 | 52 |
| LP42−195/196 | 15:50:00 | 71:41:00 | 17.3 | dM | 19.5 | DA | APO | 02-06/01 | 3600 | 0.14 | 4 | 193 | 27 |
| LP42−197 | 15:50:00 | 71:41:00 | 19.8 | dM5 | $\cdots$ | $\cdots$ | APO | 02-06/01 | 3600 | 0.14 | 4 | 280 | 4 |
| LP684−1/2 | 15:54:00 | -04:41:00 | $\cdots$ | dM | $\cdots$ | WD | CTIO | 01/02 | 780 | 0.32 | 244 | 202 | 5 |
| G152−B4A/B | 15:55:22 | -08:59:30 | 14.95 | DA5 | 14.45 | dM5 | APO | 02/01 | 600 | 0.12 | 198 | 295 | 10 |
| L266−195/196 | 16:23:00 | -54:05:00 | 11.55 | dM1 | 15.35 | DA5e | CTIO | 01/02 | 100 | 0.08 | 12 | 4 | 39 |
| LP101−15/16 | 16:33:30 | 57:15:00 | 12.91 | dM5e | 15.05 | DQ8 | APO | 09/00 | 600 | 1.62 | 319 | 23 | 26 |
| LP505−43/44 | 16:35:00 | 11:16:00 | 14.70 | dM | 18.80 | DC | APO | 09/00 | 400 | 0.17 | 159 | 77 | 60 |
| LP686−33/32 | 16:56:12 | -06:11:00 | 15.55 | dM5 | 17.21 | DC9 | APO | 09/00 | 600 | 0.35 | 111 | 211 | 110 |
| LP387−37/36 | 17:03:54 | 26:10:00 | 12.16 | dM | 17.17 | DC7 | APO | 09/00 | $\cdots$ | 0.28 | 185 | 359 | 19 |
| Wolf 672A/B | 17:16:05 | 02:00:12 | 14.36 | DA6 | 14.05 | dM5 | APO | 09/00 | 400 | 0.50 | 232 | 137 | 13 |
| LP101−409/410 | 17:16:06 | 59:51:00 | 13.01 | dM1 | 13.68 | dM0 | APO | 06/01 | 600 | 0.18 | 355 | 9 | 72 |
| LP101−411 | 17:16:06 | 59:51:00 | $\cdots$ | DA | $\cdots$ | $\cdots$ | APO | 06/01 | 600 | 0.18 | 355 | 9 | 72 |
| G154−B5A/B | 17:43:04 | -13:17:18 | 11.92 | dM3 | 14.41 | DA | APO | 09/00 | 300 | 0.09 | 25 | 32 | 33 |
| LP44−310/311 | 18:28:00 | 69:58:00 | 18.46 | DA | 18.18 | dM5 | APO | 04/01 | 3000 | 0.08 | 355 | 44 | 96 |
| LP141−12/13 | 18:56:30 | 53:27:00 | 14.4 | dM5 | 15.2 | dM5 | APO | 04/01 | 500 | 0.23 | 103 | 170 | 1 |
| LP141−14 | 18:56:30 | 53:27:00 | 18.5 | DC | $\cdots$ | $\cdots$ | $\cdots$ | $\cdots$ | $\cdots$ | 0.23 | 103 | 170 | 1 |
| LP230−20/21 | 18:59:30 | 42:56:00 | 17.71 | DC | 18.12 | dM4.5e | APO | 09/00 | 1600 | 0.26 | 201 | 51 | 15 |
| G142−B2A/B | 19:11:20 | 13:31:18 | 14.07 | DA | 12.74 | dM3 | APO | 09/00 | 300 | 0.10 | 180 | 155 | 19 |
| L923−21/22 | 19:17:54 | -07:45:00 | 12.31 | DBZ5 | 12.14 | dM5 | APO | 04/01 | 300 | 0.20 | 198 | 308 | 27 |
| LP45−217/216 | 19:23:18 | 71:31:00 | 17.32 | DA | 16.33 | dM5 | APO | 04/01 | 2100 | 0.16 | 8 | 262 | 3 |

TABLE 1 — *Continued*

| Identifier (Sp.1/Sp.2) (1) | R.A. (B1950) (2) | Decl. (B1950) (3) | $V1$ (4) | Sp.1[a] (5) | $V2$ (6) | Sp.2[a] (7) | Site (8) | U.T. (mm/yy) (9) | Exp. (sec) (10) | $\mu$ ($''$/yr) (11) | $\Theta_\mu$ (deg) (12) | Pos. (deg) (13) | Sep. ($''$) (14) |
|---|---|---|---|---|---|---|---|---|---|---|---|---|---|
| L852−36/37 | 19:32:54 | -13:36:00 | 13.60 | dM5 | 16.05 | DA5 | APO | 04/01 | 500 | 0.14 | 189 | 205 | 28 |
| LP813−18/17 | 19:43:11 | -17:26:00 | 14.64 | dM5 | 18.18 | DC | APO | 04/01 | 500 | 0.24 | 174 | 261 | 205 |
| G24−10/9 | 20:11:32 | 06:32:30 | 13.27 | dM5 | 15.78 | DQ7 | APO | 04/01 | 500 | 0.70 | 206 | 331 | 100 |
| LP575−17/18 | 20:27:36 | 06:45:00 | 17.51 | DA | 18.71 | dM4.5e | APO | 04-10/01 | 3000 | 0.22 | 32 | 29 | 77 |
| LP575−16/15 | 20:27:36 | 07:20:00 | 16.14 | DC5 | 17.18 | dM4 | APO | 04/01 | 1800 | 0.26 | 135 | 313 | 39 |
| LP46−147/148 | 20:41:00 | 73:08:00 | 18.77 | DA | 19.41 | sdM0 | APO | 10/01 | 2400 | 0.07 | 90 | 227 | 19 |
| LP696−4/5 | 20:44:42 | -04:18:00 | 17.14 | DA5 | 16.46 | dM0 | APO | 06/01 | 2400 | 0.20 | 199 | 10 | 17 |
| LP516−13/12 | 20:51:18 | 09:30:00 | 16.12 | DA | 17.02 | dM5 | APO | 07/01 | 1800 | 0.13 | 0.0 | 318 | 10 |
| Ross 193/VB11 | 20:54:06 | -05:03:00 | 11.95 | dM4e | 16.71 | DC9 | APO | 09/00 | 180 | 0.82 | 105 | 314 | 14 |
| G212−B1A/B | 21:07:59 | 42:44:48 | 15.62 | DC5 | 15.65 | dM | APO | 09/00 | 1000 | 0.20 | 98 | 310 | 22 |
| LP26−184/183 | 21:17:12 | 76:30:00 | 13.00 | dM1 | 16.47 | DA | APO | 09/00,06/01 | 300 | 0.08 | 50 | 314 | 173 |
| LP698−5/4 | 21:30:48 | -06:24:00 | 16.42 | dM2 | 18.52 | DC | APO | 09/00 | 1000 | 0.33 | 205 | 205 | 15 |
| LP187−6/7 | 21:33:27 | 46:20:18 | 16.03 | dM4.5e | 17.97 | DC | APO | 09/00 | 900 | 0.46 | 200 | 64 | 3 |
| LP398−18/19 | 21:38:30 | 21:27:00 | 16.98 | DA | 17.90 | dM5e | APO | 09/00 | 1800 | 0.12 | 195 | 100 | 81 |
| LP458−49/48 | 21:48:06 | 19:39:00 | 17.94 | DA | 18.91 | dM0 | · · · | · · · | · · · | 0.11 | 102 | 311 | 141 |
| CD−51°13128/L283−7 | 21:54:24 | -51:14:00 | 10.52 | dM0e | 14.77 | DQ7 | · · · | · · · | · · · | 0.40 | 190 | 251 | 28 |
| L427−60/61 | 21:54:48 | -43:42:00 | 14.64 | DB3 | 14.55 | dMe | · · · | · · · | · · · | 0.22 | 144 | 331 | 9 |
| LP699−29/30 | 22:01:48 | -03:46:00 | 15.95 | dM5 | 18.26 | DC9 | APO | 09/00 | 800 | 0.24 | 90 | 186 | 11 |
| LP343−35/34 | 22:13:00 | 31:43:00 | 14.64 | dM5 | 17.00 | DA | APO | 09/00 | 600 | 0.13 | 188 | 302 | 127 |
| LP188−1/2 | 22:24:11 | 48:21:42 | 17.3 | dM5 | 18.0 | DAZ | APO | 12/00,07/01 | 1500 | 0.59 | 41 | 86 | 2 |
| L573−108/109 | 22:24:36 | -34:27:00 | 14.44 | DB3 | 12.99 | dM0 | · · · | · · · | · · · | 0.21 | 94 | 15 | 9 |
| LP400−22/21 | 22:34:06 | 22:16:48 | 17.22 | DA | 17.17 | dM4.5e | APO | 09-12/00,07/01 | 2400 | 0.20 | 74 | 288 | 338 |
| LP761−113/114 | 22:49:20 | -10:32:00 | 13.50 | sdM3 | 17.39 | DA | APO | 09/00 | 300 | 0.19 | 157 | 332 | 7 |
| LP2−696/697 | 22:53:12 | 81:14:00 | 11.77 | dM0 | 17.39 | DC | APO | 09/00 | 180 | 0.23 | 63 | 134 | 8 |
| LP581−36/35 | 22:53:24 | 05:30:00 | 11.24 | dM2 | 16.19 | DA | APO | 06/01 | 180 | 0.45 | 127 | 286 | 17 |
| LP345−26/27 | 22:56:18 | 31:19:00 | 13.96 | dM | 16.75 | DA | APO | 09/00 | 400 | 0.15 | 70 | 166 | 95 |
| LP401−50/49 | 23:05:48 | 23:58:00 | 18.09 | DC | 18.14 | dM4.5e | APO | 09/00,10/01 | 2400 | 0.24 | 108 | 184 | 192 |
| LP933−66/65 | 23:09:34 | -27:37:36 | 15.47 | dM5 | 17.08 | DA | APO | 09/00 | 900 | 0.21 | 98 | 215 | 66 |
| LP522−34/35 | 23:18:00 | 12:42:00 | 16.27 | DA | 16.96 | dM5e | APO | 09/00,06/01 | 1000 | 0.18 | 72 | 50 | 35 |
| LP762−53/54 | 23:18:32 | -13:44:00 | 16.99 | dM6e | 18.79 | DC | APO | 09/00 | 1000 | 0.20 | 150 | 85 | 90 |
| LP582−42/43 | 23:19:30 | 09:30:00 | 16.24 | dM5 | 18.69 | DC | APO | 09/00 | 800 | 0.19 | 225 | 95 | 7 |
| G275−B16A/B | 23:23:30 | -24:10:54 | 15.81 | DA | 15.73 | dM0 | APO | 06-07/01 | 1800 | 0.05 | 200 | 202 | 12 |
| LP77−37A/B | 23:34:18 | 64:37:18 | 16.47 | dM5 | 20.13 | DA | APO | 09/00 | 1200 | 0.21 | 114 | 300 | 5 |
| LP463−27/26 | 23:36:24 | 20:45:00 | 14.24 | dM5e | 18.08 | DC | APO | 09/00,06/01 | 600 | 0.33 | 58 | 108 | 10 |
| LP191−9/8 | 23:41:21 | 47:09:00 | 15.32 | dM5 | 18.22 | DC | APO | 09/00 | 800 | 0.31 | 94 | 357 | 13 |
| LP347−4/5 | 23:41:24 | 32:16:12 | 12.93 | DA4 | 11.70 | dM5 | APO | 09/00 | 300 | 0.24 | 256 | 9 | 175 |
| G273−B15A/B | 23:41:45 | -16:27:30 | 14.29 | dM2 | 15.97 | DA | APO | 09/00 | 800 | 0.14 | 210 | 5 | 5 |
| LP935−14/15 | 23:44:36 | -26:39:54 | 11.29 | dM | 16.59 | DB | APO | 06/01 | 90 | 0.36 | 255 | 141 | 14 |
| LP2−246/247 | 23:48:00 | 84:31:00 | 18.90 | DC | 19.18 | dM0 | APO | 12/00,07/01 | 3600 | 0.04 | 102 | 87 | 4 |
| L577−71/72 | 23:51:31 | -33:32:48 | 14.42 | DA5 | 13.56 | dM5 | CTIO | 01/02 | 400 | 0.50 | 217 | 0 | 7 |
| LP524−35/34 | 23:54:12 | 05:23:00 | 12.45 | dM1 | 18.31 | DC | APO | 09/00 | 120 | 0.21 | 69 | 210 | 148 |
| LP348−19/20 | 23:58:54 | 27:03:00 | 17.34 | DA | 16.69 | dM5 | APO | 09/00 | 1000 | 0.11 | 106 | 122 | 10 |

NOTE. — Single-precision $V$ magnitude values are $m_{\rm pg}$ magnitudes from Luyten's original survey, all others are $V$ magnitudes from Smith (1997).

[a] Spectral types for the WD and dM stars were determined from low-resolution ($\sim$7-15 Å) spectra (Oswalt, Hintzen, & Luyten 1988; Oswalt et al. 1991, 1993). Improved dM spectral types are given in Table 3. We have made no attempt to improve upon the WD spectral types in this study.

TABLE 2
<small>Journal of the Observations.</small>

| U.T. | | | Site | Seeing | Notes |
|---|---|---|---|---|---|
| (yr) | (mo) | (day) | | (arcsec) | |
| (1) | (2) | (3) | (4) | (5) | (6) |
| 2000 | Sep | 04 | APO | ~1.0 | gibbous moon, clear |
| 2000 | Sep | 05 | APO | 1.0 | gibbous moon, clear |
| 2000 | Sep | 06 | APO | 1.0 | full moon, clear |
| 2000 | Sep | 07 | APO | 0.8 | partly cloudy |
| 2000 | Oct | 03 | APO | 0.8 | partly cloudy |
| 2000 | Dec | 06 | APO | ~1.0 | clear |
| 2001 | Jan | 24 | APO | ~3.2 | high humidity, variable seeing |
| 2001 | Jan | 25 | APO | 2.7 | high cirrus and humidity |
| 2001 | Jan | 26 | APO | 1.2 | clear |
| 2001 | Feb | 04 | APO | 0.9 | mostly cloudy |
| 2001 | Feb | 12 | APO | 0.9 | thick high cirrus |
| 2001 | Mar | 01 | APO | +2.0 | A-half: closed - hit humidity limits |
| 2001 | Apr | 01 | APO | ~1.6 | clouds, thick in west |
| 2001 | Apr | 17 | APO | 1.8 | B-half: closed - hit humidity/wind/dust limits |
| 2001 | Apr | 26 | APO | 1.4 | humidity near limits, partly cloudy |
| 2001 | Jun | 19 | APO | ~1.5 | 1$^{\rm st}$ half of A-half: closed - hit dust limits |
| 2001 | Jul | 11 | APO | 1.4 | 1$^{\rm st}$ half of A-half: closed - hit dust limits and heavy clouds |
| 2001 | Sep | 22 | APO | $\cdots$ | 1$^{\rm st}$ half of B-half: closed - hit wind limits and heavy clouds |
| 2001 | Oct | 05 | APO | ~1.5 | thick high cirrus |
| 2001 | Oct | 14 | APO | 1.9 | clear |
| 2001 | Oct | 15 | APO | 0.9 | clear |
| 2002 | Jan | 30 | CTIO | ~1.4 | gibbous moon, clear |
| 2002 | Jan | 31 | CTIO | ~1.0 | gibbous moon, clear |
| 2002 | Feb | 01 | CTIO | ~1.2 | gibbous moon, scattered high cirrus |

TABLE 3
EQUIVALENT WIDTHS AND BANDHEAD FLUX RATIOS.

| Identifier (dM) (1) | R.A. (B1950) (2) | Decl. (B1950) (3) | EW Hα (6563Å) (4) | σ_Hα (+ Å) (5) | σ_Hα (− Å) (6) | CaH1 (6385Å) (7) | CaH2 (6830Å) (8) | CaH3 (6975Å) (9) | TiO1 (6720Å) (10) | TiO2 (7059Å) (11) | TiO3 (7094Å) (12) | TiO4 (7132Å) (13) | TiO5 (7050Å) (14) | Sp.[a] (dM) (15) | Ref. (16) |
|---|---|---|---|---|---|---|---|---|---|---|---|---|---|---|---|
| LP349−14 | 00:22:06 | 27:24:00 | -0.29 | 0.02 | 0.02 | 0.85 | 0.59 | 0.81 | 0.88 | 0.81 | 0.86 | 0.81 | 0.66 | M1.0 | 3 |
| G158−77 | 00:23:28 | -10:53:30 | -0.39 | 0.02 | 0.00 | 0.91 | 0.83 | 0.92 | 0.93 | 0.91 | 0.93 | 0.87 | 0.79 | K7.5 | 3 |
| G171−B10B | 00:23:53 | 38:52:24 | -0.10 | 0.05 | 0.00 | 0.84 | 0.43 | 0.73 | 0.80 | 0.58 | 0.71 | 0.64 | 0.39 | M4.0 | 3 |
| L170−14A | 00:27:30 | -54:58:00 | 3.33 | 0.02 | 0.26 | 0.86 | 0.44 | 0.71 | 0.81 | 0.48 | 0.67 | 0.61 | 0.34 | M4.5 | 1 |
| G218−7 | 00:38:30 | 55:33:42 | -0.10 | 0.01 | 0.03 | 0.82 | 0.44 | 0.72 | 0.76 | 0.60 | 0.67 | 0.60 | 0.39 | M4.0 | 3 |
| Wolf 53 | 01:02:51 | 61:04:18 | -0.03 | 0.00 | 0.02 | 0.76 | 0.49 | 0.73 | 0.78 | 0.69 | 0.75 | 0.69 | 0.47 | M3.0 | 3 |
| LP587−54 | 01:20:42 | -02:24:48 | -0.31 | 0.01 | 0.01 | 0.87 | 0.58 | 0.80 | 0.84 | 0.76 | 0.80 | 0.75 | 0.57 | M2.0 | 3 |
| G34−48 | 01:42:31 | 23:02:48 | -0.19 | 0.00 | 0.01 | 0.86 | 0.65 | 0.82 | 0.88 | 0.82 | 0.85 | 0.81 | 0.67 | M0.5 | 3 |
| LP352−31 | 01:45:06 | 21:32:00 | -0.17 | 0.02 | 0.02 | 0.84 | 0.50 | 0.76 | 0.82 | 0.69 | 0.73 | 0.67 | 0.48 | M3.0 | 3 |
| G244−37 | 01:48:12 | 64:11:24 | -0.21 | 0.04 | 0.00 | 0.84 | 0.56 | 0.78 | 0.84 | 0.72 | 0.78 | 0.72 | 0.53 | M2.5 | 3 |
| G71−B5A | 01:50:31 | 08:56:42 | -0.27 | 0.03 | 0.02 | 0.87 | 0.56 | 0.79 | 0.85 | 0.72 | 0.80 | 0.74 | 0.57 | M2.0 | 3 |
| G272−B2B | 01:58:32 | -16:00:36 | -0.05 | 0.04 | 0.01 | 0.80 | 0.48 | 0.70 | 0.77 | 0.69 | 0.72 | 0.72 | 0.46 | M3.0 | 3 |
| LP885−23 | 02:04:51 | -30:38:30 | -0.07 | 0.00 | 0.00 | 0.82 | 0.51 | 0.74 | 0.82 | 0.67 | 0.73 | 0.69 | 0.50 | M2.5 | 3 |
| LP590−142 | 02:25:52 | 00:24:30 | -0.19 | 0.05 | 0.03 | 0.85 | 0.43 | 0.71 | 0.81 | 0.59 | 0.67 | 0.64 | 0.39 | M4.0 | 3 |
| LP355−11 | 02:57:42 | 24:42:00 | -0.05 | 0.02 | 0.03 | 0.81 | 0.44 | 0.73 | 0.79 | 0.60 | 0.68 | 0.65 | 0.40 | M3.5 | 3 |
| LP472−38 | 03:17:18 | 11:24:00 | -0.12 | 0.04 | 0.01 | 0.78 | 0.60 | 0.78 | 0.86 | 0.82 | 0.85 | 0.80 | 0.64 | M1.0 | 3 |
| LP31−140 | 03:24:30 | 73:15:00 | 0.20 | 0.06 | 0.00 | 0.82 | 0.41 | 0.70 | 0.77 | 0.54 | 0.64 | 0.60 | 0.33 | M4.5 | 1 |
| LP356−87 | 03:25:00 | 26:21:00 | -0.10 | 0.01 | 0.00 | 0.83 | 0.55 | 0.79 | 0.82 | 0.74 | 0.79 | 0.76 | 0.54 | M2.0 | 3 |
| LP773−12 | 03:31:48 | -16:05:00 | 0.11 | 0.01 | 0.00 | 0.82 | 0.48 | 0.73 | 0.80 | 0.69 | 0.72 | 0.69 | 0.47 | M3.0 | 2 |
| LP31−276 | 03:54:36 | 70:47:00 | -0.21 | 0.02 | 0.00 | 0.87 | 0.65 | 0.83 | 0.87 | 0.85 | 0.86 | 0.85 | 0.69 | M0.5 | 3 |
| LP889−21 | 03:58:00 | -32:06:00 | -0.14 | 0.01 | 0.01 | 0.81 | 0.45 | 0.75 | 0.72 | 0.62 | 0.69 | 0.61 | 0.40 | M3.5 | 3 |
| LP415−1 | 04:17:12 | 19:47:00 | -0.02 | 0.03 | 0.04 | 0.81 | 0.44 | 0.71 | 0.78 | 0.62 | 0.70 | 0.67 | 0.45 | M3.0 | 3 |
| LP775−52 | 04:19:26 | -16:07:06 | -0.24 | 0.00 | 0.00 | 0.85 | 0.64 | 0.82 | 0.85 | 0.85 | 0.86 | 0.83 | 0.68 | M0.5 | 3 |
| G175−34A | 04:26:50 | 58:53:18 | 0.07 | 0.04 | 0.01 | 0.85 | 0.46 | 0.73 | 0.80 | 0.58 | 0.67 | 0.62 | 0.36 | M4.0 | 2 |
| HZ 9B | 04:29:24 | 17:38:00 | 6.97 | 0.05 | 0.03 | 0.86 | 0.55 | 0.73 | 0.87 | 0.64 | 0.76 | 0.77 | 0.50 | M2.5 | 1 |
| LP891−13 | 04:43:18 | -27:32:00 | 3.08 | 0.04 | 0.74 | 0.83 | 0.45 | 0.67 | 0.82 | 0.54 | 0.77 | 0.66 | 0.38 | M4.0 | 1 |
| G86−B1A | 05:18:26 | 33:19:12 | 0.02 | 0.03 | 0.01 | 0.80 | 0.52 | 0.76 | 0.81 | 0.71 | 0.78 | 0.71 | 0.55 | M2.0 | 2 |
| LP779−20 | 06:04:18 | -19:50:00 | 0.30 | 0.01 | 0.10 | 0.74 | 0.35 | 0.64 | 0.58 | 0.58 | 0.60 | 0.55 | 0.35 | M4.5 | 2 |
| LP600−43 | 06:28:08 | -02:03:42 | 0.06 | 0.01 | 0.02 | 0.81 | 0.44 | 0.71 | 0.79 | 0.65 | 0.66 | 0.62 | 0.43 | M3.5 | 2 |
| LP205−28 | 06:41:50 | 43:48:36 | 0.26 | 0.04 | 0.01 | 0.92 | 0.45 | 0.77 | 0.76 | 0.65 | 0.66 | 0.65 | 0.43 | M3.5 | 1 |
| G87−28 | 07:06:52 | 37:45:24 | -0.08 | 0.05 | 0.03 | 0.78 | 0.41 | 0.69 | 0.76 | 0.56 | 0.64 | 0.59 | 0.35 | M4.5 | 3 |
| LP422−7 | 07:09:18 | 19:24:00 | -0.01 | 0.01 | 0.00 | 0.77 | 0.44 | 0.70 | 0.78 | 0.69 | 0.75 | 0.67 | 0.45 | M3.0 | 3 |
| LP207−8 | 07:26:06 | 39:17:00 | -0.10 | 0.01 | 0.02 | 0.84 | 0.51 | 0.74 | 0.84 | 0.71 | 0.86 | 0.67 | 0.51 | M2.5 | 3 |
| G107−69 | 07:27:02 | 48:19:06 | -0.26 | 0.05 | 0.04 | 0.81 | 0.41 | 0.70 | 0.76 | 0.56 | 0.65 | 0.58 | 0.36 | M4.0 | 3 |
| LP783−2 | 07:38:02 | -17:17:24 | -0.01 | 0.05 | 0.04 | 0.79 | 0.23 | 0.57 | 0.63 | 0.30 | 0.45 | 0.39 | 0.14 | M6.5 | 3 |
| LP366−2 | 07:41:37 | 24:50:24 | -0.07 | 0.00 | 0.01 | 0.83 | 0.56 | 0.82 | 0.81 | 0.76 | 0.80 | 0.77 | 0.57 | M2.0 | 3 |
| LP208−33 | 08:04:18 | 44:40:00 | -0.23 | 0.03 | 0.03 | 0.81 | 0.47 | 0.72 | 0.81 | 0.65 | 0.74 | 0.65 | 0.46 | M3.0 | 3 |
| LP664−16 | 08:06:30 | -04:23:00 | -0.15 | 0.02 | 0.00 | 0.86 | 0.61 | 0.82 | 0.83 | 0.80 | 0.83 | 0.80 | 0.63 | M1.0 | 3 |
| LP163−120 | 08:07:24 | 48:25:00 | -0.16 | 0.04 | 0.04 | 0.86 | 0.52 | 0.77 | 0.82 | 0.69 | 0.78 | 0.67 | 0.50 | M2.5 | 3 |
| G111−72 | 08:16:47 | 38:44:18 | -0.22 | 0.03 | 0.00 | 0.85 | 0.63 | 0.84 | 0.85 | 0.80 | 0.82 | 0.78 | 0.62 | M1.5 | 3 |
| L186−120 | 08:20:42 | -58:32:00 | -0.39 | 0.01 | 0.04 | 0.89 | 0.56 | 0.79 | 0.91 | 0.78 | 0.95 | 0.78 | 0.51 | M2.5 | 3 |
| LP164−51[b] | 08:42:48 | 49:37:00 | 1.22 | 0.02 | 0.18 | 0.56 | 0.38 | 0.54 | 0.74 | 0.79 | 0.81 | 0.69 | 0.60 | 1.5 | 1 |
| LP844−25 | 08:51:42 | -24:36:00 | 0.66 | 0.03 | 0.02 | 0.62 | 0.21 | 0.47 | 0.65 | 0.41 | 0.48 | 0.42 | 0.22 | M6.0 | 2 |
| LP90−71 | 08:55:40 | 60:28:18 | 0.01 | 0.02 | 0.01 | 0.82 | 0.44 | 0.72 | 0.75 | 0.61 | 0.66 | 0.64 | 0.38 | M4.0 | 2 |
| LP845−9 | 08:58:42 | -22:02:00 | -0.24 | 0.03 | 0.00 | 0.83 | 0.61 | 0.82 | 0.83 | 0.83 | 0.85 | 0.80 | 0.67 | M0.5 | 3 |
| LP60−177 | 08:59:30 | 68:17:00 | -0.15 | 0.00 | 0.00 | 0.88 | 0.72 | 0.86 | 0.90 | 0.90 | 0.92 | 0.92 | 0.82 | K7.0 | 3 |
| LP313−13 | 09:04:30 | 27:49:00 | 2.98 | 0.06 | 0.01 | 0.79 | 0.40 | 0.68 | 0.73 | 0.51 | 0.60 | 0.61 | 0.34 | M4.5 | 1 |
| LP313−15 | 09:06:18 | 29:42:00 | -0.12 | 0.01 | 0.01 | 0.82 | 0.58 | 0.80 | 0.81 | 0.80 | 0.83 | 0.77 | 0.59 | M1.5 | 3 |
| LP60−237 | 09:11:24 | 65:09:00 | -0.21 | 0.00 | 0.01 | 0.91 | 0.70 | 0.86 | 0.85 | 0.85 | 0.87 | 0.87 | 0.72 | M0.0 | 3 |
| LP487−26 | 09:16:00 | 11:11:00 | 0.04 | 0.00 | 0.04 | 0.84 | 0.38 | 0.70 | 0.71 | 0.52 | 0.62 | 0.53 | 0.31 | M4.5 | 1 |
| LP787−25 | 09:18:30 | -17:16:00 | 0.16 | 0.00 | 0.08 | 1.06 | 0.56 | 0.87 | 1.08 | 1.19 | 1.15 | 1.19 | 0.72 | M0.0 | 2 |
| G117−B15B | 09:21:13 | 35:29:48 | 2.64 | 0.00 | 0.01 | 0.78 | 0.41 | 0.67 | 0.75 | 0.60 | 0.67 | 0.65 | 0.39 | M4.0 | 1 |

TABLE 3 — *Continued*

| Identifier (dM) (1) | R.A. (B1950) (2) | Decl. (B1950) (3) | EW Hα (6563Å) (4) | σ_Hα (+ Å) (5) | σ_Hα (− Å) (6) | CaH1 (6385Å) (7) | CaH2 (6830Å) (8) | CaH3 (6975Å) (9) | TiO1 (6720Å) (10) | TiO2 (7059Å) (11) | TiO3 (7094Å) (12) | TiO4 (7132Å) (13) | TiO5 (7050Å) (14) | Sp.[a] (dM) (15) | Ref. (16) |
|---|---|---|---|---|---|---|---|---|---|---|---|---|---|---|---|
| G161−37 | 09:26:51 | -03:57:00 | -0.11 | 0.00 | 0.02 | 0.79 | 0.46 | 0.71 | 0.78 | 0.68 | 0.72 | 0.66 | 0.46 | M3.0 | 3 |
| LP488−20 | 09:37:42 | 09:21:00 | 0.00 | 0.02 | 0.01 | 0.77 | 0.38 | 0.66 | 0.71 | 0.62 | 0.68 | 0.59 | 0.35 | M4.5 | 3 |
| LP370−40 | 09:41:00 | 22:34:00 | 0.07 | 0.01 | 0.01 | 0.79 | 0.42 | 0.70 | 0.69 | 0.63 | 0.67 | 0.66 | 0.40 | M3.5 | 1 |
| G117−B11A | 09:43:23 | 33:05:18 | -0.25 | 0.02 | 0.02 | 0.80 | 0.45 | 0.71 | 0.79 | 0.66 | 0.74 | 0.65 | 0.45 | M3.0 | 3 |
| LP62−34A | 10:04:36 | 66:34:00 | -0.55 | 0.01 | 0.01 | 0.98 | 0.89 | 0.93 | 0.97 | 0.94 | 0.97 | 0.93 | 0.89 | K6.5 | 3 |
| LP847−41 | 10:10:18 | -23:58:00 | -0.28 | 0.00 | 0.05 | 0.92 | 0.66 | 0.82 | 0.92 | 0.81 | 0.96 | 0.80 | 0.58 | M1.5 | 3 |
| CD-18:3019 | 10:43:30 | -18:50:00 | -0.22 | 0.00 | 0.00 | 0.86 | 0.66 | 0.85 | 0.87 | 0.87 | 0.88 | 0.85 | 0.70 | M0.5 | 3 |
| LP317−25 | 10:54:24 | 30:30:00 | -0.16 | 0.02 | 0.02 | 0.88 | 0.65 | 0.82 | 0.89 | 0.81 | 0.86 | 0.81 | 0.68 | M0.5 | 3 |
| LP214−39 | 11:05:12 | 41:16:00 | -0.45 | 0.01 | 0.01 | 0.95 | 0.83 | 0.92 | 0.95 | 0.93 | 0.97 | 0.93 | 0.86 | K6.5 | 3 |
| LP672−2 | 11:05:30 | -04:53:00 | -0.10 | 0.01 | 0.01 | 0.85 | 0.48 | 0.75 | 0.80 | 0.70 | 0.74 | 0.70 | 0.47 | M3.0 | 3 |
| LP373−85 | 11:08:48 | 25:30:00 | 0.29 | 0.01 | 0.01 | 0.81 | 0.42 | 0.70 | 0.78 | 0.62 | 0.70 | 0.62 | 0.38 | M4.0 | 1 |
| LP792−6 | 11:11:30 | -18:47:00 | -0.03 | 0.03 | 0.06 | 0.86 | 0.43 | 0.73 | 0.78 | 0.55 | 0.67 | 0.59 | 0.37 | M4.0 | 3 |
| LP552−48 | 11:20:54 | 07:18:00 | -0.46 | 0.01 | 0.01 | 0.96 | 0.84 | 0.93 | 0.92 | 0.92 | 0.94 | 0.90 | 0.79 | K7/M0 | 3 |
| LP906−23 | 11:20:54 | -32:07:00 | -0.32 | 0.01 | 0.02 | 0.92 | 0.60 | 0.80 | 0.88 | 0.70 | 0.84 | 0.73 | 0.49 | M2.5 | 3 |
| LP906−34 | 11:32:54 | -29:53:00 | -0.06 | 0.05 | 0.00 | 1.00 | 0.66 | 0.89 | 1.05 | 1.22 | 1.11 | 1.11 | 0.86 | K6.5 | 3 |
| G148−6 | 11:43:21 | 32:06:12 | 0.10 | 0.01 | 0.04 | 0.81 | 0.44 | 0.70 | 0.79 | 0.60 | 0.70 | 0.63 | 0.43 | M3.5 | 1 |
| LP375−50 | 11:47:46 | 25:35:18 | 9.60 | 0.01 | 0.00 | 0.78 | 0.45 | 0.68 | 0.80 | 0.58 | 0.70 | 0.70 | 0.41 | M3.5 | 1 |
| LP493−61 | 11:48:48 | 13:11:00 | -0.21 | 0.00 | 0.01 | 0.86 | 0.65 | 0.85 | 0.84 | 0.83 | 0.84 | 0.82 | 0.62 | M1.5 | 3 |
| LP129−586 | 11:48:48 | 54:28:00 | 0.07 | 0.02 | 0.01 | 0.79 | 0.45 | 0.70 | 0.78 | 0.70 | 0.74 | 0.72 | 0.48 | M3.0 | 2 |
| LP216−75 | 12:11:06 | 39:18:00 | -0.18 | 0.00 | 0.01 | 0.90 | 0.76 | 0.88 | 0.90 | 0.92 | 0.94 | 0.93 | 0.84 | K7.0 | 3 |
| LP554−64 | 12:14:18 | 03:14:00 | -0.27 | 0.01 | 0.04 | 0.84 | 0.46 | 0.73 | 0.80 | 0.60 | 0.71 | 0.63 | 0.43 | M3.5 | 3 |
| LP435−59 | 12:20:24 | 19:06:00 | -0.11 | 0.04 | 0.06 | 0.82 | 0.47 | 0.73 | 0.77 | 0.62 | 0.73 | 0.65 | 0.44 | M3.5 | 3 |
| LP795−14 | 12:22:48 | -16:50:00 | 0.18 | 0.02 | 0.03 | 0.82 | 0.51 | 0.78 | 0.78 | 0.74 | 0.72 | 0.71 | 0.49 | M2.5 | 2 |
| LP495−176 | 12:30:36 | 12:16:00 | -0.04 | 0.05 | 0.05 | 0.89 | 0.48 | 0.76 | 0.80 | 0.62 | 0.72 | 0.65 | 0.46 | M3.0 | 3 |
| LP321−205 | 12:30:42 | 26:22:00 | -0.01 | 0.04 | 0.06 | 0.85 | 0.42 | 0.73 | 0.63 | 0.59 | 0.62 | 0.63 | 0.39 | M4.0 | 3 |
| G61−16 | 12:44:44 | 14:58:24 | -0.30 | 0.01 | 0.02 | 0.84 | 0.66 | 0.84 | 0.88 | 0.87 | 0.91 | 0.86 | 0.76 | K7/M0 | 3 |
| LP497−29 | 13:11:30 | 11:14:00 | -0.13 | 0.07 | 0.03 | 0.83 | 0.36 | 0.69 | 0.73 | 0.53 | 0.65 | 0.59 | 0.34 | M4.5 | 3 |
| HZ 43B | 13:14:00 | 29:22:00 | 1.42 | 0.00 | 0.03 | 0.93 | 0.70 | 0.81 | 0.90 | 0.70 | 0.83 | 0.81 | 0.64 | M1.0 | 1 |
| LP617−34 | 13:17:42 | -02:08:00 | 6.55 | 0.08 | 0.06 | 0.81 | 0.38 | 0.69 | 0.78 | 0.51 | 0.63 | 0.62 | 0.34 | M4.5 | 1 |
| G14−57 | 13:27:40 | -08:18:48 | -0.17 | 0.04 | 0.03 | 0.84 | 0.39 | 0.71 | 0.76 | 0.53 | 0.64 | 0.58 | 0.35 | M4.5 | 3 |
| LP798−14 | 13:34:18 | -16:04:00 | 2.29 | 0.05 | 0.03 | 0.84 | 0.53 | 0.76 | 0.87 | 0.73 | 0.81 | 0.76 | 0.61 | M1.5 | 1 |
| LP738−42 | 13:34:48 | -11:48:00 | -0.35 | 0.02 | 0.04 | 0.86 | 0.48 | 0.76 | 0.80 | 0.60 | 0.71 | 0.64 | 0.42 | M3.5 | 3 |
| LP498−25 | 13:36:45 | 12:23:48 | -0.28 | 0.00 | 0.05 | 0.86 | 0.53 | 0.78 | 0.83 | 0.68 | 0.77 | 0.69 | 0.51 | M2.5 | 3 |
| LP219−78 | 13:48:18 | 41:48:00 | 0.22 | 0.08 | 0.03 | 0.86 | 0.36 | 0.66 | 0.79 | 0.55 | 0.66 | 0.58 | 0.33 | M4.5 | 1 |
| LP856−54 | 13:48:30 | -27:19:00 | -0.27 | 0.03 | 0.01 | 0.85 | 0.59 | 0.81 | 0.86 | 0.79 | 0.83 | 0.79 | 0.63 | M1.0 | 3 |
| LP439−180 | 14:00:42 | 16:04:00 | -0.12 | 0.03 | 0.02 | 0.76 | 0.38 | 0.69 | 0.77 | 0.55 | 0.65 | 0.61 | 0.33 | M4.5 | 3 |
| LP133−373[c] | 14:02:24 | 50:36:00 | 7.70 | 0.08 | 0.07 | 0.80 | 0.41 | 0.66 | 0.77 | 0.55 | 0.67 | 0.64 | 0.37 | M4.0 | 1 |
| LP799−74 | 14:09:36 | -18:29:00 | 0.27 | 0.07 | 0.00 | 0.75 | 0.35 | 0.64 | 0.76 | 0.54 | 0.66 | 0.58 | 0.36 | M4.0 | 1 |
| LP66−587 | 14:16:06 | 63:18:00 | -0.10 | 0.03 | 0.00 | 0.80 | 0.56 | 0.78 | 0.84 | 0.78 | 0.81 | 0.77 | 0.63 | M1.0 | 3 |
| G200−40 | 14:25:59 | 54:01:00 | -0.27 | 0.02 | 0.01 | 0.92 | 0.80 | 0.90 | 0.93 | 0.91 | 0.93 | 0.90 | 0.81 | K7.0 | 3 |
| LP135−155 | 15:10:34 | 56:36:12 | 0.03 | 0.02 | 0.02 | 0.76 | 0.45 | 0.73 | 0.79 | 0.66 | 0.71 | 0.64 | 0.42 | M3.5 | 2 |
| LP223−14 | 15:25:30 | 43:23:30 | -0.14 | 0.03 | 0.03 | 0.78 | 0.53 | 0.78 | 0.81 | 0.75 | 0.76 | 0.69 | 0.57 | M2.0 | 3 |
| LP176−59 | 15:33:12 | 46:59:00 | -0.41 | 0.09 | 0.01 | 0.79 | 0.28 | 0.59 | 0.67 | 0.40 | 0.53 | 0.46 | 0.23 | M5.5 | 3 |
| LP743−25 | 15:39:12 | -13:47:00 | -0.05 | 0.08 | 0.01 | 0.72 | 0.35 | 0.65 | 0.71 | 0.53 | 0.65 | 0.61 | 0.37 | M4.0 | 3 |
| LP916−26 | 15:42:18 | -27:30:00 | -0.17 | 0.05 | 0.02 | 0.83 | 0.39 | 0.69 | 0.79 | 0.56 | 0.68 | 0.62 | 0.38 | M4.0 | 3 |
| G152−B4A | 15:55:22 | -08:59:30 | -0.05 | 0.03 | 0.02 | 0.81 | 0.52 | 0.77 | 0.81 | 0.73 | 0.75 | 0.71 | 0.50 | M2.5 | 3 |
| LP101−15 | 16:33:30 | 57:15:00 | 1.91 | 0.05 | 0.15 | 0.81 | 0.39 | 0.66 | 0.79 | 0.51 | 0.69 | 0.57 | 0.34 | M4.5 | 1 |
| LP505−43 | 16:35:00 | 11:16:00 | -0.18 | 0.05 | 0.03 | 0.82 | 0.51 | 0.77 | 0.87 | 0.74 | 0.83 | 0.73 | 0.60 | M1.5 | 3 |
| LP686−33 | 16:56:12 | -06:11:00 | 0.19 | 0.02 | 0.01 | 0.74 | 0.42 | 0.67 | 0.77 | 0.64 | 0.71 | 0.64 | 0.43 | M3.5 | 2 |
| LP387−37 | 17:03:54 | 26:10:00 | -0.23 | 0.02 | 0.02 | 0.85 | 0.61 | 0.82 | 0.86 | 0.76 | 0.82 | 0.76 | 0.61 | M1.5 | 3 |
| Wolf 672B | 17:16:05 | 02:00:12 | -0.19 | 0.07 | 0.02 | 0.85 | 0.40 | 0.71 | 0.80 | 0.56 | 0.68 | 0.61 | 0.40 | M3.5 | 3 |
| G154−B5A | 17:43:04 | -13:17:18 | -0.11 | 0.02 | 0.03 | 0.90 | 0.68 | 0.85 | 0.94 | 0.87 | 0.94 | 0.88 | 0.80 | K7/M0 | 3 |
| LP44−311 | 18:28:00 | 69:58:00 | -0.33 | 0.02 | 0.04 | 0.83 | 0.45 | 0.72 | 0.85 | 0.69 | 0.73 | 0.63 | 0.45 | M3.0 | 3 |
| LP230−21 | 18:59:30 | 42:56:00 | 0.04 | 0.00 | 0.00 | 0.79 | 0.32 | 0.65 | 0.75 | 0.44 | 0.59 | 0.50 | 0.25 | M5.5 | 2 |

TABLE 3 — *Continued*

| Identifier (dM) (1) | R.A. (B1950) (2) | Decl. (B1950) (3) | EW Hα (6563Å) (4) | σ$_{H\alpha}$ (+ Å) (5) | σ$_{H\alpha}$ (− Å) (6) | CaH1 (6385Å) (7) | CaH2 (6830Å) (8) | CaH3 (6975Å) (9) | TiO1 (6720Å) (10) | TiO2 (7059Å) (11) | TiO3 (7094Å) (12) | TiO4 (7132Å) (13) | TiO5 (7050Å) (14) | Sp.[a] (dM) (15) | Ref. (16) |
|---|---|---|---|---|---|---|---|---|---|---|---|---|---|---|---|
| G142−B2B | 19:11:20 | 13:31:18 | -0.19 | 0.04 | 0.01 | 0.82 | 0.51 | 0.76 | 0.84 | 0.75 | 0.80 | 0.75 | 0.58 | M1.5 | 3 |
| L923−22 | 19:17:54 | -07:45:00 | -0.14 | 0.02 | 0.04 | 0.77 | 0.44 | 0.71 | 0.80 | 0.67 | 0.73 | 0.69 | 0.50 | M2.5 | 3 |
| LP45−216 | 19:23:18 | 71:31:00 | -0.17 | 0.01 | 0.01 | 0.77 | 0.47 | 0.71 | 0.80 | 0.70 | 0.75 | 0.70 | 0.49 | M2.5 | 3 |
| L852−36 | 19:32:54 | -13:36:00 | -0.41 | 0.02 | 0.04 | 0.89 | 0.70 | 0.87 | 0.92 | 0.84 | 0.91 | 0.86 | 0.77 | K7/M0 | 3 |
| LP813−18 | 19:43:11 | -17:26:00 | -0.42 | 0.04 | 0.03 | 0.85 | 0.50 | 0.76 | 0.81 | 0.69 | 0.81 | 0.72 | 0.50 | M2.5 | 3 |
| G24−10 | 20:11:32 | 06:32:30 | -0.12 | 0.03 | 0.03 | 0.83 | 0.43 | 0.74 | 0.79 | 0.59 | 0.69 | 0.64 | 0.42 | M3.5 | 3 |
| LP575−18 | 20:27:36 | 06:45:00 | -0.23 | 0.18 | 0.13 | 0.76 | 0.28 | 0.54 | 0.69 | 0.40 | 0.61 | 0.53 | 0.24 | M5.5 | 3 |
| LP575−15 | 20:27:36 | 07:20:00 | -0.33 | 0.02 | 0.04 | 0.79 | 0.32 | 0.65 | 0.80 | 0.50 | 0.60 | 0.57 | 0.32 | M4.5 | 3 |
| LP698−5 | 20:44:42 | -04:18:00 | -0.06 | 0.04 | 0.01 | 0.82 | 0.41 | 0.71 | 0.78 | 0.63 | 0.71 | 0.64 | 0.44 | M3.5 | 3 |
| Ross 193 | 20:54:06 | -05:03:00 | 1.61 | 0.04 | 0.03 | 0.81 | 0.42 | 0.69 | 0.80 | 0.57 | 0.67 | 0.62 | 0.39 | M4.0 | 1 |
| G212−B1B | 21:07:59 | 42:44:48 | -0.01 | 0.02 | 0.03 | 0.79 | 0.46 | 0.71 | 0.77 | 0.69 | 0.72 | 0.66 | 0.44 | M3.5 | 3 |
| LP26−184 | 21:17:12 | 76:30:00 | -0.37 | 0.03 | 0.01 | 0.99 | 0.83 | 0.92 | 0.92 | 0.94 | 0.97 | 0.96 | 0.90 | K6.0 | 3 |
| LP696−5 | 21:30:48 | -06:24:00 | -0.20 | 0.04 | 0.01 | 0.77 | 0.41 | 0.69 | 0.80 | 0.63 | 0.72 | 0.64 | 0.46 | M3.0 | 3 |
| LP187−6 | 21:33:27 | 46:20:18 | -0.15 | 0.00 | 0.03 | 0.87 | 0.41 | 0.73 | 0.78 | 0.56 | 0.63 | 0.56 | 0.33 | M4.5 | 3 |
| LP398−19 | 21:38:30 | 21:27:00 | -0.05 | 0.03 | 0.02 | 0.85 | 0.46 | 0.73 | 0.83 | 0.65 | 0.71 | 0.66 | 0.42 | M3.5 | 3 |
| LP699−29 | 22:01:48 | -03:46:00 | -0.29 | 0.06 | 0.01 | 0.79 | 0.50 | 0.73 | 0.76 | 0.69 | 0.77 | 0.70 | 0.52 | M2.5 | 3 |
| LP343−35 | 22:13:00 | 31:43:00 | -0.16 | 0.01 | 0.01 | 0.85 | 0.51 | 0.76 | 0.81 | 0.67 | 0.75 | 0.70 | 0.47 | M3.0 | 3 |
| LP400−21 | 22:34:06 | 22:16:48 | -0.14 | 0.03 | 0.02 | 0.78 | 0.41 | 0.67 | 0.77 | 0.59 | 0.67 | 0.62 | 0.38 | M4.0 | 3 |
| LP2−696 | 22:53:12 | 81:14:00 | -0.35 | 0.01 | 0.03 | 0.90 | 0.81 | 0.91 | 0.91 | 0.85 | 0.90 | 0.84 | 0.73 | M0.0 | 3 |
| LP581−36 | 22:53:24 | 05:30:00 | -0.35 | 0.04 | 0.02 | 0.87 | 0.58 | 0.82 | 0.87 | 0.81 | 0.83 | 0.81 | 0.65 | M1.0 | 3 |
| LP401−49 | 23:05:48 | 23:58:00 | -0.17 | 0.07 | 0.04 | 0.79 | 0.36 | 0.68 | 0.77 | 0.46 | 0.60 | 0.55 | 0.30 | M5.0 | 3 |
| LP933−66 | 23:09:34 | -27:37:36 | -0.27 | 0.03 | 0.05 | 0.82 | 0.49 | 0.75 | 0.83 | 0.68 | 0.75 | 0.68 | 0.50 | M2.5 | 3 |
| LP522−35 | 23:18:00 | 12:42:00 | -0.44 | 0.05 | 0.06 | 0.86 | 0.47 | 0.73 | 0.80 | 0.58 | 0.74 | 0.62 | 0.41 | M3.5 | 3 |
| LP762−53 | 23:18:32 | -13:44:00 | 13.38 | 0.05 | 0.09 | 0.85 | 0.42 | 0.69 | 0.80 | 0.45 | 0.67 | 0.65 | 0.33 | M4.5 | 1 |
| LP582−42 | 23:19:30 | 09:30:00 | -0.12 | 0.00 | 0.02 | 0.79 | 0.45 | 0.71 | 0.78 | 0.62 | 0.71 | 0.65 | 0.42 | M3.5 | 3 |
| LP77−37A | 23:34:18 | 64:37:18 | 0.11 | 0.03 | 0.00 | 0.79 | 0.40 | 0.69 | 0.77 | 0.66 | 0.70 | 0.67 | 0.42 | M3.5 | 2 |
| LP463−27 | 23:36:24 | 20:45:00 | 4.83 | 0.19 | 0.06 | 0.78 | 0.38 | 0.64 | 0.78 | 0.55 | 0.69 | 0.65 | 0.39 | M4.0 | 1 |
| LP191−9 | 23:41:21 | 47:09:00 | 0.05 | 0.03 | 0.02 | 0.77 | 0.42 | 0.71 | 0.80 | 0.71 | 0.74 | 0.70 | 0.47 | M3.0 | 2 |
| LP347−5 | 23:41:24 | 32:16:12 | -0.09 | 0.04 | 0.01 | 0.80 | 0.45 | 0.73 | 0.80 | 0.69 | 0.75 | 0.70 | 0.49 | M2.5 | 3 |
| G273−B15A | 23:41:45 | -16:27:30 | -0.14 | 0.03 | 0.00 | 0.83 | 0.58 | 0.80 | 0.88 | 0.81 | 0.85 | 0.81 | 0.67 | M0.5 | 3 |
| LP935−14 | 23:44:36 | -26:39:54 | -0.47 | 0.03 | 0.01 | 0.97 | 0.75 | 0.89 | 0.96 | 0.89 | 0.94 | 0.91 | 0.82 | K7.0 | 3 |
| L577−72 | 23:51:31 | -33:32:48 | -0.40 | 0.01 | 0.01 | 0.87 | 0.64 | 0.79 | 0.88 | 0.73 | 0.82 | 0.76 | 0.60 | M1.5 | 3 |
| LP524−35 | 23:54:12 | 05:23:00 | -0.39 | 0.01 | 0.00 | 0.92 | 0.87 | 0.91 | 0.89 | 0.90 | 0.92 | 0.89 | 0.80 | K7/M0 | 3 |
| LP348−20 | 23:58:54 | 27:03:00 | -0.30 | 0.02 | 0.03 | 0.81 | 0.50 | 0.75 | 0.80 | 0.66 | 0.71 | 0.67 | 0.47 | M3.0 | 3 |

REFERENCES. — (1) dMe Stars; (2) dM(e) Stars; (3) dM Stars.

[a] Improved dM spectral types based on TiO5 bandhead ratios.
[b] Stellar halo white dwarf candidate.
[c] M dwarf has close (eclipsing) companion.

TABLE 4
Parameters for the dMe and dM(e) Stars.

| Identifier (dM) (1) | R.A. (B1950) (2) | Decl. (B1950) (3) | $V - I$ (4) | $M_V$ (5) | Mass ($M_\odot$) (6) |
|---|---|---|---|---|---|
| dMe Stars | | | | | |
| L170−14A | 00:27:30 | -54:58:00 | 3.30 | 13.51 | 0.18 |
| LP31−140 | 03:24:30 | 73:15:00 | 3.09 | 13.01 | 0.21 |
| HZ 9B | 04:29:24 | 17:38:00 | 2.52 | 11.34 | 0.34 |
| LP891−13 | 04:43:18 | -27:32:00 | 2.86 | 13.00 | 0.21 |
| LP205−28 | 06:41:50 | 43:48:36 | 2.59 | 11.55 | 0.32 |
| LP313−13 | 09:04:30 | 27:49:00 | 3.07 | 12.94 | 0.21 |
| LP487−26 | 09:16:00 | 11:11:00 | 3.23 | 13.35 | 0.19 |
| G117−B15B | 09:21:13 | 35:29:48 | 2.77 | 12.11 | 0.27 |
| LP370−40 | 09:41:00 | 22:34:00 | 2.82 | 12.27 | 0.26 |
| LP373−85 | 11:08:48 | 25:30:00 | 2.92 | 13.00 | 0.21 |
| G148−6 | 11:43:21 | 32:06:12 | 2.67 | 11.80 | 0.30 |
| LP375−50 | 11:47:46 | 25:35:18 | 2.71 | 11.93 | 0.29 |
| HZ 43B | 13:14:00 | 29:22:00 | 2.04 | 9.75 | 0.52 |
| LP617−34 | 13:17:42 | -02:08:00 | 2.94 | 13.00 | 0.21 |
| LP798−14 | 13:34:18 | -16:04:00 | 2.18 | 10.22 | 0.46 |
| LP219−78 | 13:48:18 | 41:48:00 | 2.07 | 9.83 | 0.51 |
| LP133−373 | 14:02:24 | 50:36:00 | 2.87 | 13.00 | 0.21 |
| LP799−74 | 14:09:36 | -18:29:00 | 3.08 | 12.97 | 0.21 |
| LP101−15 | 16:33:30 | 57:15:00 | 2.88 | 13.00 | 0.21 |
| Ross 193 | 20:54:06 | -05:03:00 | 2.72 | 11.97 | 0.28 |
| LP762−53 | 23:18:32 | -13:44:00 | 3.15 | 13.15 | 0.20 |
| LP463−27 | 23:36:24 | 20:45:00 | 2.76 | 12.07 | 0.28 |
| dM(e) Stars | | | | | |
| LP773−12 | 03:31:48 | -16:05:00 | 2.55 | 11.45 | 0.33 |
| G175−34A | 04:26:50 | 58:53:18 | 2.86 | 13.00 | 0.21 |
| G86−B1A | 05:18:26 | 33:19:12 | 2.37 | 10.87 | 0.39 |
| LP779−20 | 06:04:18 | -19:50:00 | 3.17 | 13.21 | 0.20 |
| LP600−43 | 06:28:08 | -02:03:42 | 3.15 | 13.15 | 0.20 |
| LP844−25 | 08:51:42 | -24:36:00 | 3.76 | 14.35 | 0.15 |
| LP90−71 | 08:55:40 | 60:28:18 | 2.77 | 12.12 | 0.27 |
| LP787−25 | 09:18:30 | -17:16:00 | 3.24 | 13.36 | 0.19 |
| LP129−586 | 11:48:48 | 54:28:00 | 2.53 | 11.36 | 0.55 |
| LP795−14 | 12:22:48 | -16:50:00 | 2.39 | 10.92 | 0.38 |
| LP135−155 | 15:10:34 | 56:36:12 | 2.59 | 11.55 | 0.32 |
| LP686−33 | 16:56:12 | -06:11:00 | 2.74 | 12.02 | 0.28 |
| LP230−21 | 18:59:30 | 42:56:00 | 3.71 | 14.27 | 0.15 |
| LP77−37A | 23:34:18 | 64:37:18 | 2.78 | 12.14 | 0.27 |
| LP191−9 | 23:41:21 | 47:09:00 | 2.47 | 11.20 | 0.36 |

TABLE 5
Complete Space Motions for 161 M Dwarf Stars.

| Identifier (dM) (1) | R.A. (B1950) (2) | Decl. (B1950) (3) | $\mu$ (″/yr) (4) | $\Theta$ (deg) (5) | $v_r$ (km/s) (6) | $\sigma_{v_r}$ (km/s) (7) | $U$ (km/s) (8) | $\sigma_U$ (km/s) (9) | $V$ (km/s) (10) | $\sigma_V$ (km/s) (11) | $W$ (km/s) (12) | $\sigma_W$ (km/s) (13) | Sp.V. (km/s) (14) | $\sigma_{\text{Sp.V.}}$ (km/s) (15) | Ref. (16) |
|---|---|---|---|---|---|---|---|---|---|---|---|---|---|---|---|
| LP349−14 | 00.3683 | 27.4000 | 0.12 | 90 | 48.6 | 3.5 | 37.2 | 0.9 | 7.4 | 1.9 | -38.2 | 2.8 | 53.8 | 0.1 | 3 |
| G158−77 | 00.3911 | -10.8917 | 0.27 | 160 | 52.2 | 6.4 | -27.6 | 0.9 | -110.5 | 3.2 | -93.5 | 5.5 | 147.3 | 0.0 | 3 |
| G171−B10B | 00.3981 | 38.8733 | 0.20 | 132 | 19.4 | 2.9 | 20.1 | 0.9 | -22.5 | 1.8 | -46.0 | 2.1 | 55.0 | 0.0 | 3 |
| L170−14A | 00.4583 | -54.8917 | 0.36 | 240 | 16.2 | 14.8 | -43.8 | 6.0 | -16.4 | 9.9 | -11.9 | 9.2 | 48.2 | 0.2 | 1 |
| G218−8 | 00.6417 | 55.5589 | 0.32 | 103 | 20.5 | 8.5 | 21.2 | 3.5 | -7.5 | 5.7 | -15.9 | 5.2 | 27.5 | 0.2 | 3 |
| LP825−712 | 00.6767 | -22.0333 | 0.50 | 83 | 11.9 | 30.0 | 53.1 | 7.2 | -39.8 | 16.0 | -20.3 | 24.3 | 69.4 | 0.3 | 4 |
| LP242−11 | 00.8750 | 32.5333 | 0.50 | 242 | 22.8 | 33.6 | -159.5 | 10.6 | 58.1 | 19.3 | -96.8 | 25.4 | 195.4 | 0.1 | 2,4 |
| LP1−169 | 01.0167 | 86.6667 | 0.13 | 73 | 23.7 | 5.1 | 11.6 | 2.5 | -1.7 | 3.8 | 6.5 | 2.4 | 13.4 | 0.3 | 2,4 |
| Wolf 53 | 01.0475 | 61.0717 | 0.48 | 137 | 23.9 | 25.7 | 76.0 | 11.3 | -44.4 | 17.8 | -92.7 | 14.7 | 127.9 | 0.1 | 3 |
| LP587−54 | 01.3450 | -02.4133 | 0.22 | 79 | 9.8 | 8.9 | 22.6 | 2.7 | -23.4 | 4.4 | -9.3 | 7.3 | 33.8 | 0.2 | 3 |
| G34−48 | 01.7086 | 23.0467 | 0.32 | 112 | 32.9 | 7.4 | 58.5 | 3.0 | -58.3 | 4.0 | -34.8 | 5.5 | 89.6 | 0.1 | 3 |
| LP352−31 | 01.7517 | 21.5333 | 0.20 | 80 | 15.3 | 7.3 | 54.6 | 3.0 | -39.4 | 3.9 | 6.9 | 5.5 | 67.7 | 0.1 | 3 |
| G244−37 | 01.8033 | 64.1900 | 0.29 | 129 | 14.3 | 7.6 | 14.3 | 3.6 | -12.2 | 5.3 | -15.2 | 4.1 | 24.2 | 0.2 | 3 |
| G71−B5A | 01.8419 | 08.9450 | 0.10 | 154 | 31.3 | 6.7 | 6.6 | 2.8 | -26.0 | 3.3 | -42.8 | 5.1 | 50.5 | 0.1 | 3 |
| G272−B2B | 01.9756 | -16.0100 | 0.13 | 81 | 16.6 | 19.8 | 35.7 | 8.7 | -36.6 | 10.1 | -8.4 | 14.7 | 51.8 | 0.3 | 3 |
| LP885−23 | 02.0808 | -30.6417 | 0.25 | 124 | 16.9 | 14.1 | 2.1 | 6.5 | -50.4 | 7.9 | -13.7 | 9.7 | 52.2 | 0.2 | 3 |
| LP245−18 | 02.2892 | 37.5633 | 0.35 | 102 | 5.8 | 8.6 | 74.2 | 4.2 | -97.4 | 5.1 | 8.4 | 5.5 | 122.8 | 0.1 | 2,4 |
| LP590−142 | 02.4311 | 00.4083 | 0.11 | 155 | 13.9 | 8.3 | -8.6 | 4.3 | -56.6 | 4.0 | -31.3 | 5.9 | 65.3 | 0.1 | 3 |
| LP355−11 | 02.9617 | 24.7000 | 0.18 | 124 | -26.5 | 8.9 | 3.2 | 5.3 | -100.9 | 4.7 | 4.5 | 5.4 | 101.0 | 0.1 | 3 |
| LP472−38 | 03.2883 | 11.4000 | 0.18 | 192 | 9.7 | 6.6 | -31.5 | 4.3 | -50.9 | 3.2 | -60.7 | 3.8 | 85.2 | 0.1 | 3,4 |
| LP355−64 | 03.3250 | 26.9833 | 0.18 | 124 | 27.6 | 25.2 | 65.9 | 16.0 | -135.1 | 13.5 | -12.6 | 14.0 | 150.8 | 0.1 | 3,4 |
| LP31−140 | 03.4083 | 73.8500 | 0.43 | 141 | 0.0 | 7.7 | 66.1 | 3.9 | -73.5 | 5.6 | -33.7 | 3.6 | 104.5 | 0.1 | 1 |
| LP356−87 | 03.4167 | 26.3500 | 0.18 | 120 | -10.8 | 6.7 | -4.0 | 4.3 | -50.5 | 3.6 | 2.3 | 3.6 | 50.7 | 0.1 | 3 |
| LP888−63 | 03.4458 | -27.3100 | 0.83 | 63 | 17.0 | 25.4 | 14.3 | 16.5 | -24.8 | 13.7 | -9.7 | 13.7 | 30.2 | 0.6 | 3,4 |
| LP773−12 | 03.5300 | -16.0833 | 0.32 | 80 | 14.0 | 9.3 | 44.9 | 6.4 | -57.8 | 4.6 | 30.6 | 5.0 | 79.3 | 0.1 | 2 |
| LP31−276 | 03.9100 | 70.7833 | 0.17 | 74 | 5.1 | 7.4 | 4.1 | 3.8 | -31.2 | 5.3 | 29.1 | 3.4 | 42.9 | 0.1 | 3 |
| LP889−21 | 03.9683 | -32.1000 | 0.21 | 117 | 13.3 | 13.6 | -5.6 | 9.4 | -71.0 | 7.6 | 17.3 | 6.4 | 73.3 | 0.1 | 3 |
| LP415−1 | 04.2867 | 19.7833 | 0.17 | 216 | -23.1 | 7.0 | -52.7 | 5.3 | -30.0 | 3.5 | -59.8 | 2.9 | 85.2 | 0.1 | 3 |
| LP775−52 | 04.3239 | -16.1183 | 0.35 | 112 | 37.8 | 5.9 | 17.4 | 4.6 | -79.4 | 2.9 | 2.6 | 2.4 | 81.3 | 0.1 | 3 |
| G175−34A | 04.4489 | 58.8667 | 2.37 | 146 | 2.1 | 9.8 | 17.9 | 5.7 | -49.4 | 6.7 | -14.2 | 4.3 | 54.5 | 0.1 | 2 |
| HZ 9B | 04.4900 | 17.6333 | 0.12 | 110 | -10.4 | 9.8 | -17.8 | 7.7 | -16.7 | 4.8 | -0.9 | 3.8 | 24.4 | 0.3 | 1 |
| LP358−52B | 04.5483 | 26.9333 | 0.11 | 108 | 23.4 | 6.0 | 14.5 | 4.5 | -12.5 | 3.2 | -10.4 | 2.3 | 21.8 | 0.2 | 3,4 |
| LP891−13 | 04.7217 | -27.5333 | 0.24 | 246 | 22.2 | 41.2 | -15.9 | 31.5 | -13.1 | 21.9 | -47.4 | 15.1 | 51.7 | 0.6 | 1 |
| G86−B1A | 05.3072 | 33.3200 | 0.18 | 113 | 52.4 | 9.3 | 47.6 | 7.1 | -40.2 | 5.2 | 12.8 | 3.0 | 63.6 | 0.1 | 2 |
| LP159−33 | 05.8664 | 46.8483 | 0.54 | 179 | 36.7 | 37.0 | 29.6 | 25.6 | -13.0 | 23.1 | -5.7 | 13.3 | 32.8 | 0.8 | 3 |
| LP779−20 | 06.0717 | -19.8333 | 0.23 | 108 | 24.8 | 10.8 | -29.4 | 9.0 | -103.1 | 5.3 | 69.1 | 2.6 | 127.5 | 0.1 | 2 |
| LP600−43 | 06.4689 | -02.0617 | 0.25 | 214 | -14.9 | 7.9 | -33.4 | 6.8 | -17.0 | 3.6 | -36.9 | 1.7 | 52.6 | 0.1 | 2 |
| LP205−28 | 06.6972 | 43.8100 | 0.12 | 176 | -11.8 | 8.4 | 9.4 | 5.9 | -138.3 | 5.1 | -49.2 | 3.1 | 147.1 | 0.0 | 1 |
| G87−28 | 07.1144 | 37.7567 | 0.44 | 222 | -4.6 | 10.2 | 4.4 | 7.4 | -39.8 | 5.9 | -57.8 | 3.8 | 70.4 | 0.1 | 3 |
| LP422−7 | 07.1550 | 19.4000 | 0.10 | 147 | -4.2 | 7.9 | -26.9 | 6.3 | -50.0 | 3.9 | -2.1 | 2.6 | 56.8 | 0.1 | 3 |
| LP5−74 | 07.4333 | 82.7333 | 0.18 | 76 | 14.4 | 7.8 | -51.2 | 3.8 | -13.4 | 5.8 | 76.7 | 3.6 | 93.2 | 0.1 | ⋯ |
| LP207−8 | 07.4350 | 39.2833 | 0.12 | 186 | 44.3 | 9.6 | 38.8 | 6.7 | -52.5 | 5.7 | -5.0 | 3.9 | 65.5 | 0.1 | 3 |
| G107−69 | 07.4506 | 48.3183 | 1.34 | 191 | -0.9 | 10.6 | 17.2 | 6.9 | -82.4 | 6.7 | -36.4 | 4.5 | 91.7 | 0.1 | 3 |
| LP783−2 | 07.6342 | -17.2900 | 1.26 | 117 | -10.0 | 13.5 | -115.5 | 10.4 | -72.9 | 6.6 | 72.5 | 5.5 | 154.7 | 0.1 | 3 |
| LP366−2 | 07.6936 | 24.8400 | 0.10 | 260 | -13.1 | 6.6 | -2.3 | 4.9 | -4.9 | 3.4 | -53.1 | 2.8 | 53.3 | 0.1 | 3 |
| LP208−33 | 08.0717 | 44.6667 | 0.10 | 200 | 3.9 | 8.6 | 2.9 | 5.4 | -34.5 | 5.3 | -15.8 | 4.0 | 38.1 | 0.2 | 3 |
| LP664−16 | 08.1083 | -04.3833 | 0.12 | 182 | 18.8 | 6.9 | -9.0 | 5.1 | -41.8 | 3.2 | -14.5 | 3.3 | 45.1 | 0.1 | 3 |
| LP163−120 | 08.1233 | 48.4167 | 0.14 | 79 | 17.9 | 9.5 | -30.0 | 5.8 | -9.1 | 6.0 | 57.4 | 4.5 | 65.4 | 0.1 | 3 |
| G111−72 | 08.2797 | 38.7383 | 0.38 | 212 | 19.9 | 6.5 | 30.7 | 4.2 | -65.2 | 3.8 | -35.3 | 3.2 | 80.3 | 0.1 | 3 |
| L186−120 | 08.3450 | -58.5333 | 0.20 | 289 | 51.0 | ⋯ | 40.2 | ⋯ | -56.4 | ⋯ | -57.1 | ⋯ | 89.8 | ⋯ | 3 |
| LP164−51[a] | 08.7133 | 49.6167 | 0.31 | 159 | 24.0 | 12.3 | -0.7 | 7.0 | -136.6 | 7.9 | 48.7 | 6.3 | 145.0 | 0.1 | 1,4 |
| LP844−25 | 08.8617 | -24.6000 | 0.64 | 78 | -0.1 | 15.9 | -89.4 | 9.8 | -6.9 | 8.4 | 137.1 | 9.3 | 163.8 | 0.1 | 2 |
| LP60−359B | 08.8733 | 63.0500 | 0.11 | 110 | 22.1 | 18.8 | -0.5 | 9.8 | -9.1 | 13.1 | 17.6 | 9.3 | 19.8 | 0.7 | 1 |

TABLE 5 — *Continued*

| Identifier (dM) (1) | R.A. (B1950) (2) | Decl. (B1950) (3) | $\mu$ ($''$/yr) (4) | $\Theta$ (deg) (5) | $v_r$ (km/s) (6) | $\sigma_{v_r}$ (km/s) (7) | $U$ (km/s) (8) | $\sigma_U$ (km/s) (9) | $V$ (km/s) (10) | $\sigma_V$ (km/s) (11) | $W$ (km/s) (12) | $\sigma_W$ (km/s) (13) | Sp.V. (km/s) (14) | $\sigma_{\mathrm{Sp.V.}}$ (km/s) (15) | Ref. (16) |
|---|---|---|---|---|---|---|---|---|---|---|---|---|---|---|---|
| LP90−71 | 08.9278 | 60.4717 | 0.53 | 216 | -0.8 | 8.1 | 68.2 | 4.2 | -108.1 | 5.6 | -46.3 | 4.1 | 135.9 | 0.0 | 2 |
| LP845−9 | 08.9783 | -22.0333 | 0.19 | 319 | 26.8 | 6.6 | 72.3 | 4.0 | -8.8 | 3.4 | -2.5 | 4.0 | 72.9 | 0.1 | 3 |
| LP60−177 | 08.9917 | 68.2833 | 0.16 | 215 | 12.9 | 5.5 | 83.6 | 2.8 | -96.2 | 3.9 | -24.9 | 2.7 | 129.9 | 0.0 | 3 |
| LP313−13 | 09.0750 | 27.8167 | 0.13 | 160 | 11.1 | 10.9 | -20.4 | 6.4 | -60.4 | 5.9 | 4.6 | 6.6 | 63.9 | 0.1 | 1 |
| LP313−15 | 09.1050 | 29.7000 | 0.14 | 237 | 24.0 | 7.0 | 49.9 | 4.0 | -61.5 | 3.9 | -50.4 | 4.2 | 93.9 | 0.1 | 3 |
| LP60−237 | 09.1900 | 65.1500 | 0.14 | 241 | 17.6 | 7.7 | 44.0 | 3.9 | -30.0 | 5.4 | -23.6 | 3.9 | 58.3 | 0.1 | 3 |
| LP487−26 | 09.2667 | 11.1833 | 0.35 | 235 | 8.6 | 10.0 | 34.4 | 5.7 | -69.9 | 4.9 | -84.4 | 6.6 | 114.9 | 0.1 | 1 |
| LP787−25 | 09.3083 | -17.2667 | 0.20 | 323 | -10.4 | 37.0 | 55.8 | 20.8 | 26.4 | 18.7 | -6.9 | 24.3 | 62.1 | 0.4 | 3 |
| G117−B15B | 09.3536 | 35.4967 | 0.14 | 264 | 2.3 | 9.4 | 20.3 | 5.0 | -17.6 | 5.5 | -33.1 | 5.8 | 42.7 | 0.2 | 1 |
| G161−37 | 09.4475 | -03.9500 | 0.27 | 274 | 13.8 | 9.9 | 47.4 | 5.4 | -21.8 | 4.7 | -42.5 | 6.8 | 67.3 | 0.1 | 0 |
| LP488−20 | 09.6283 | 09.3500 | 0.26 | 255 | 10.1 | 10.2 | 40.6 | 5.2 | -38.5 | 5.0 | -52.4 | 7.2 | 76.6 | 0.1 | 2 |
| LP370−40 | 09.6833 | 22.5667 | 0.12 | 201 | -21.8 | 8.0 | -21.1 | 4.0 | -71.6 | 4.2 | -53.3 | 5.5 | 91.7 | 0.1 | 1 |
| G117−B11A | 09.7231 | 33.0883 | 0.14 | 133 | 10.9 | 9.4 | -24.1 | 4.6 | -33.3 | 5.4 | 15.6 | 6.2 | 44.0 | 0.2 | 3 |
| LP62−34A | 10.0767 | 66.5667 | 0.21 | 224 | 22.7 | 11.1 | 59.8 | 5.3 | -65.9 | 7.9 | 0.5 | 5.8 | 88.9 | 0.1 | 3 |
| LP847−41 | 10.1717 | -23.9667 | 0.18 | 312 | 60.2 | $\cdots$ | 83.4 | $\cdots$ | -52.6 | $\cdots$ | 23.3 | $\cdots$ | 101.3 | 7.0 | 3 |
| CD−18°3019 | 10.7250 | -18.8333 | 1.98 | 250 | 40.3 | 6.5 | 123.4 | 2.1 | -134.4 | 3.4 | -125.5 | 5.2 | 221.5 | 0.0 | 3 |
| LP317−25 | 10.9067 | 30.5000 | 0.16 | 270 | 36.0 | 7.8 | 80.4 | 2.6 | -42.6 | 4.4 | -11.7 | 5.9 | 91.7 | 0.1 | 3 |
| LP214−39 | 11.0867 | 41.2667 | 0.21 | 275 | 34.7 | 9.2 | 57.6 | 3.3 | -24.1 | 5.7 | 0.8 | 6.5 | 62.4 | 0.1 | 3 |
| LP672−2 | 11.0917 | -04.8833 | 0.44 | 184 | 24.0 | 7.1 | -23.7 | 1.6 | -55.7 | 3.5 | -10.7 | 6.0 | 61.5 | 0.1 | 3 |
| LP373−85 | 11.1467 | 25.5833 | 0.24 | 266 | 13.5 | 11.1 | 60.3 | 3.1 | -45.3 | 6.1 | -24.0 | 8.8 | 79.2 | 0.1 | 1 |
| LP792−6 | 11.1917 | -18.7833 | 0.25 | 300 | 24.6 | 9.4 | 31.7 | 2.3 | -32.7 | 4.9 | 9.5 | 7.7 | 46.5 | 0.1 | 3 |
| LP552−48 | 11.3483 | 07.3000 | 0.20 | 110 | 39.5 | 8.7 | -77.4 | 1.5 | -25.6 | 4.3 | 42.1 | 7.4 | 91.8 | 0.1 | 3 |
| LP906−23 | 11.3483 | -32.1167 | 0.24 | 282 | 64.1 | $\cdots$ | 11.9 | $\cdots$ | -77.8 | $\cdots$ | 16.7 | $\cdots$ | 80.4 | $\cdots$ | 3 |
| LP906−34 | 11.5483 | -29.8833 | 0.16 | 227 | 70.6 | $\cdots$ | -6.5 | $\cdots$ | -98.8 | $\cdots$ | -10.9 | $\cdots$ | 99.7 | $\cdots$ | 3 |
| LP493−16 | 11.5633 | 08.3167 | 0.25 | 245 | 25.6 | 17.4 | 24.0 | 2.4 | -58.8 | 8.7 | -4.5 | 14.9 | 63.6 | 0.2 | 3 |
| G148−6 | 11.7225 | 32.1033 | 0.28 | 203 | 23.3 | 10.7 | -4.5 | 2.9 | -50.5 | 6.2 | 14.0 | 8.3 | 52.6 | 0.1 | 1 |
| LP375−50 | 11.7961 | 25.5883 | 0.30 | 252 | 14.7 | 10.9 | 44.9 | 2.4 | -64.1 | 6.0 | -10.2 | 8.8 | 78.9 | 0.1 | 1 |
| LP493−61 | 11.8133 | 13.1833 | 0.21 | 182 | 27.7 | 21.5 | -44.2 | 2.9 | -93.4 | 10.9 | -2.9 | 18.3 | 103.3 | 0.2 | 3 |
| LP129−586 | 11.8133 | 54.4667 | 0.25 | 264 | 6.0 | 6.1 | 94.9 | 2.4 | -72.3 | 4.1 | -24.1 | 3.8 | 121.7 | 0.0 | 2 |
| LP673−42A | 11.8453 | -07.0933 | 0.54 | 198 | 28.9 | 17.4 | -18.3 | 1.7 | -57.7 | 8.7 | -6.1 | 15.0 | 60.9 | 0.2 | 3 |
| LP554−64 | 12.2383 | 03.2333 | 0.70 | 293 | 31.1 | 10.5 | 45.1 | 1.0 | -33.2 | 5.2 | 23.2 | 9.1 | 60.6 | 0.1 | 3 |
| LP320−644 | 12.2517 | 32.3667 | 0.26 | 234 | 15.1 | 7.3 | 12.1 | 2.0 | -52.2 | 4.2 | 5.3 | 5.6 | 53.8 | 0.1 | 3,4 |
| LP435−59 | 12.3400 | 19.1000 | 0.19 | 268 | 14.2 | 7.2 | 68.5 | 1.3 | -62.2 | 3.8 | -3.6 | 6.0 | 92.6 | 0.1 | 3 |
| LP795−14 | 12.3800 | -16.8333 | 0.12 | 211 | 46.0 | 8.9 | -13.5 | 1.6 | -118.4 | 4.6 | -40.2 | 7.5 | 125.7 | 0.1 | 2 |
| LP495−176 | 12.5100 | 12.2667 | 0.16 | 284 | 25.2 | 13.5 | 62.1 | 2.2 | -41.4 | 6.8 | 16.8 | 11.4 | 76.5 | 0.1 | 3 |
| LP321−205 | 12.5117 | 26.3667 | 0.15 | 263 | -3.5 | 12.0 | 65.6 | 3.0 | -70.0 | 6.6 | -17.4 | 9.6 | 97.5 | 0.1 | 3 |
| G61−16 | 12.7456 | 14.9733 | 0.43 | 298 | 20.2 | 5.2 | 134.7 | 1.1 | -28.9 | 2.7 | 25.4 | 4.3 | 140.1 | 0.0 | 3 |
| LP497−30 | 13.1917 | 11.2333 | 0.24 | 207 | -22.5 | 6.2 | -14.2 | 1.8 | -97.8 | 3.1 | -47.9 | 5.1 | 109.8 | 0.0 | 3 |
| HZ 43B | 13.2333 | 29.3667 | 0.16 | 240 | 44.4 | 14.4 | 160.7 | 4.9 | -396.0 | 8.1 | 79.6 | 10.9 | 434.7 | 0.0 | 1,4 |
| LP617−34 | 13.2950 | -02.1333 | 0.19 | 159 | 7.3 | 8.5 | -29.0 | 2.5 | -25.8 | 4.2 | -12.6 | 7.0 | 40.8 | 0.2 | 1 |
| G14−57 | 13.4581 | -08.3133 | 1.24 | 247 | 35.7 | 4.8 | 37.0 | 1.6 | -118.0 | 2.4 | 11.4 | 3.9 | 124.2 | 0.0 | 3 |
| LP798−14 | 13.5717 | -16.0667 | 0.12 | 246 | 54.1 | 2.7 | -21.2 | 1.0 | -61.1 | 1.4 | 27.9 | 2.1 | 70.4 | 0.0 | 1 |
| LP738−42 | 13.5800 | -11.8000 | 0.19 | 199 | 35.1 | 9.3 | -34.2 | 3.4 | -81.1 | 4.7 | -15.4 | 7.3 | 89.4 | 0.1 | 3,4 |
| LP498−25 | 13.6125 | 12.3967 | 0.19 | 134 | 50.3 | 9.1 | -63.7 | 3.4 | -21.3 | 4.6 | 27.5 | 7.1 | 72.6 | 0.1 | 3 |
| LP219−78 | 13.8050 | 41.8000 | 0.14 | 160 | 24.9 | 22.9 | -217.6 | 10.1 | -111.4 | 14.1 | 49.1 | 15.0 | 249.3 | 0.1 | 1 |
| LP856−54 | 13.8083 | -27.3167 | 0.24 | 199 | 49.9 | 4.3 | -38.8 | 1.8 | -71.0 | 2.4 | -9.2 | 3.1 | 81.5 | 0.0 | 3 |
| LP439−180 | 14.0117 | 16.0667 | 0.08 | 167 | 9.5 | 8.7 | -32.1 | 3.9 | -28.0 | 4.4 | -5.1 | 6.4 | 42.9 | 0.1 | 3 |
| LP133−373[b] | 14.0400 | 50.6000 | 0.20 | 308 | 14.0 | 9.9 | 19.0 | 4.7 | -9.0 | 6.5 | 5.4 | 5.9 | 21.7 | 0.3 | 1 |
| LP799−74 | 14.1600 | -18.4833 | 0.19 | 133 | 29.8 | 6.1 | -59.6 | 2.9 | -22.8 | 3.1 | -18.6 | 4.4 | 66.5 | 0.1 | 1 |
| LP66−587 | 14.2683 | 63.3000 | 0.09 | 140 | 13.2 | 18.9 | -61.8 | 9.2 | -1.1 | 13.2 | 14.3 | 9.9 | 63.5 | 0.2 | 3 |
| G200−40 | 14.4330 | 54.0167 | 0.39 | 294 | 33.7 | 7.8 | 78.2 | 3.9 | -29.8 | 5.2 | 38.2 | 4.4 | 91.9 | 0.1 | 3 |
| LP135−155 | 15.1761 | 56.6033 | 0.38 | 217 | 13.6 | 9.8 | -54.1 | 5.3 | -98.6 | 6.6 | 80.6 | 5.0 | 138.3 | 0.1 | 2 |
| LP223−14 | 15.4250 | 43.3917 | 0.14 | 186 | 32.5 | 5.1 | -246.9 | 3.1 | -163.1 | 3.1 | 77.0 | 2.6 | 305.7 | 0.0 | 3 |
| LP176−59 | 15.5533 | 46.9833 | 0.51 | 296 | 11.5 | 10.6 | 89.6 | 6.3 | -54.7 | 6.7 | 58.0 | 5.3 | 120.0 | 0.1 | 3 |

TABLE 5 — *Continued*

| Identifier (dM) (1) | R.A. (B1950) (2) | Decl. (B1950) (3) | $\mu$ (''/yr) (4) | $\Theta$ (deg) (5) | $v_r$ (km/s) (6) | $\sigma_{v_r}$ (km/s) (7) | $U$ (km/s) (8) | $\sigma_U$ (km/s) (9) | $V$ (km/s) (10) | $\sigma_V$ (km/s) (11) | $W$ (km/s) (12) | $\sigma_W$ (km/s) (13) | Sp.V. (km/s) (14) | $\sigma_{\text{Sp.V.}}$ (km/s) (15) | Ref. (16) |
|---|---|---|---|---|---|---|---|---|---|---|---|---|---|---|---|
| LP743−25 | 15.6533 | -13.7833 | 0.20 | 314 | 34.6 | 11.9 | 12.6 | 8.4 | -11.5 | 5.8 | 93.7 | 6.2 | 95.2 | 0.1 | 3 |
| L480−84 | 15.7592 | -38.1667 | 0.09 | 162 | 79.4 | ⋯ | -82.2 | ⋯ | -58.5 | ⋯ | -25.8 | ⋯ | 104.1 | ⋯ | 3 |
| LP916−26 | 15.7003 | -27.5000 | 0.24 | 235 | -8.1 | 6.7 | 11.9 | 4.5 | -50.9 | 3.6 | -5.9 | 3.4 | 52.6 | 0.1 | 3 |
| LP42−195 | 15.8333 | 71.6833 | 0.14 | 4 | 2.5 | 9.3 | -2.8 | 4.8 | -9.0 | 6.7 | -8.7 | 4.3 | 12.8 | 0.5 | 2 |
| G152−B4A | 15.9228 | -08.9917 | 0.12 | 198 | 36.2 | 17.8 | -45.6 | 13.2 | -37.0 | 8.4 | 3.3 | 8.5 | 58.8 | 0.2 | 3 |
| L266−195 | 16.3833 | -54.0833 | 0.08 | 12 | 74.4 | ⋯ | -81.6 | ⋯ | -35.4 | ⋯ | -2.5 | ⋯ | 88.9 | ⋯ | 3 |
| LP101−15 | 16.5583 | 57.2500 | 1.62 | 319 | 3.4 | 12.5 | 57.0 | 7.5 | -28.3 | 8.4 | 21.5 | 5.4 | 67.2 | 0.1 | 1 |
| LP505−43 | 16.5833 | 11.2667 | 0.17 | 159 | 1.3 | 2.2 | -49.1 | 1.8 | -35.2 | 1.0 | -40.3 | 0.8 | 72.6 | 0.0 | 3 |
| LP686−33 | 16.9367 | -06.1833 | 0.35 | 111 | -24.8 | 9.0 | -12.1 | 7.5 | 6.3 | 4.1 | -92.9 | 2.7 | 93.9 | 0.1 | 2 |
| LP387−37 | 17.0650 | 26.1667 | 0.28 | 185 | 3.9 | 6.7 | -40.6 | 5.3 | -30.9 | 3.5 | -11.1 | 2.2 | 52.2 | 0.1 | 3 |
| Wolf 672B | 17.2681 | 02.0033 | 0.50 | 232 | -19.0 | 1.9 | -7.3 | 1.6 | -73.9 | 0.9 | 8.4 | 0.5 | 74.7 | 0.0 | 3 |
| LP101−409 | 17.2683 | 59.8500 | 0.18 | 355 | 4.4 | 21.7 | 46.5 | 13.0 | -7.1 | 14.8 | -4.5 | 9.1 | 47.2 | 0.3 | 3 |
| LP101−410 | 17.2683 | 59.8500 | 0.18 | 355 | 3.7 | 18.8 | 43.0 | 11.3 | -7.8 | 12.8 | -4.9 | 7.8 | 44.0 | 0.3 | 3 |
| G154−B5A | 17.7178 | -13.2883 | 0.09 | 25 | -2.2 | 3.8 | -2.7 | 3.3 | 3.8 | 1.8 | -5.6 | 0.8 | 7.3 | 0.4 | 3 |
| LP44−311 | 18.4667 | 69.9667 | 0.08 | 355 | 29.7 | 9.5 | 109.5 | 5.2 | -16.9 | 6.8 | 25.5 | 4.2 | 113.7 | 0.1 | 3 |
| LP230−21 | 18.9917 | 42.9333 | 0.26 | 201 | -10.2 | 11.4 | -75.8 | 8.0 | -41.8 | 6.9 | -11.5 | 4.3 | 87.3 | 0.1 | 2 |
| G142−B2B | 19.1889 | 13.5217 | 0.10 | 180 | 2.7 | 1.9 | -21.0 | 1.6 | -19.1 | 0.9 | -14.1 | 0.6 | 31.7 | 0.0 | 3 |
| L923−22 | 19.2983 | -07.7500 | 0.20 | 198 | 36.1 | 13.3 | -46.9 | 10.9 | -7.7 | 6.2 | -15.4 | 4.6 | 50.0 | 0.2 | 3 |
| LP45−216 | 19.3883 | 71.5167 | 0.16 | 8 | 33.2 | 9.8 | 66.2 | 5.2 | -2.8 | 7.1 | 16.7 | 4.4 | 68.3 | 0.1 | 3 |
| L852−36 | 19.5483 | -13.6000 | 0.14 | 189 | 54.0 | 4.8 | -75.4 | 3.8 | -40.1 | 2.3 | -36.7 | 1.9 | 92.9 | 0.0 | 3 |
| LP813−18 | 19.7197 | -17.4333 | 0.24 | 174 | 47.5 | 7.4 | -60.0 | 5.7 | -39.9 | 3.6 | -47.4 | 3.1 | 86.2 | 0.1 | 3 |
| G24−10 | 20.1922 | 06.5417 | 0.70 | 206 | 30.0 | 5.5 | -71.7 | 4.0 | -30.1 | 2.6 | -19.4 | 2.7 | 80.1 | 0.1 | 3 |
| LP575−18 | 20.4600 | 06.7500 | 0.22 | 32 | 54.2 | 25.5 | 21.1 | 17.8 | 78.3 | 12.0 | -24.3 | 13.8 | 84.7 | 0.2 | 3 |
| LP575−15 | 20.4600 | 70.3333 | 0.26 | 135 | 27.9 | 3.7 | -12.3 | 1.9 | 37.2 | 2.7 | -61.1 | 1.7 | 72.6 | 0.0 | 3 |
| LP696−5 | 20.7450 | -04.3000 | 0.20 | 199 | 26.0 | 5.0 | -83.1 | 3.3 | -68.2 | 2.4 | -33.0 | 2.9 | 112.5 | 0.0 | 3 |
| Ross 193 | 20.9017 | -04.9500 | 0.82 | 105 | -8.1 | 11.1 | 15.9 | 7.0 | -23.1 | 5.3 | -35.4 | 6.8 | 45.1 | 0.2 | 1 |
| G212−B1B | 21.1331 | 42.7356 | 0.20 | 98 | 2.2 | 6.9 | 26.4 | 3.8 | -10.2 | 4.2 | -57.6 | 3.9 | 64.2 | 0.1 | 3 |
| LP26−184 | 21.2867 | 76.5000 | 0.08 | 50 | 12.5 | 26.0 | 36.9 | 12.7 | -15.2 | 19.0 | -9.2 | 12.3 | 40.9 | 0.5 | 3 |
| LP696−5 | 21.5133 | -06.4000 | 0.33 | 205 | -2.5 | 3.8 | -120.4 | 2.0 | -128.5 | 1.8 | -16.9 | 2.7 | 176.9 | 0.0 | 3 |
| LP187−6 | 21.5575 | 46.3383 | 0.46 | 200 | 3.1 | 8.5 | -92.3 | 4.3 | -9.7 | 5.4 | -51.2 | 5.0 | 106.0 | 0.1 | 3 |
| LP398−19 | 21.6417 | 21.4500 | 0.12 | 195 | -0.8 | 7.0 | -88.9 | 3.5 | -54.8 | 3.7 | -52.9 | 4.8 | 117.0 | 0.0 | 3 |
| LP699−29 | 22.0300 | -03.7667 | 0.24 | 90 | 1.5 | 9.1 | 83.9 | 4.0 | -28.7 | 4.4 | -77.9 | 6.9 | 118.0 | 0.1 | 3 |
| LP343−35 | 22.2167 | 31.7167 | 0.13 | 188 | 5.3 | 8.2 | -31.5 | 3.5 | -15.6 | 4.7 | -30.4 | 5.8 | 46.4 | 0.1 | 3 |
| LP188−1 | 22.4031 | 48.3617 | 0.59 | 41 | -10.8 | 8.0 | 18.2 | 3.5 | -26.3 | 5.2 | 3.3 | 5.1 | 32.1 | 0.2 | 3 |
| LP400−21 | 22.5683 | 22.2800 | 0.20 | 74 | 7.4 | 9.1 | 75.0 | 3.2 | -14.9 | 4.8 | -35.5 | 7.0 | 84.3 | 0.1 | 3 |
| LP761−113 | 22.8222 | -10.5333 | 0.19 | 157 | 20.5 | 1.7 | -17.9 | 0.5 | -40.7 | 0.9 | -44.1 | 1.4 | 62.6 | 0.0 | 3 |
| LP2−696 | 22.8867 | 81.2333 | 0.23 | 63 | 34.1 | 10.0 | 44.8 | 4.8 | -4.6 | 7.4 | 4.4 | 4.7 | 45.3 | 0.2 | 3 |
| LP581−36 | 22.8900 | 05.5000 | 0.45 | 127 | 51.6 | 1.6 | 0.0 | 0.4 | -4.6 | 0.8 | -72.6 | 1.3 | 72.7 | 0.0 | 3 |
| LP345−26 | 22.9383 | 31.3167 | 0.15 | 70 | 26.5 | 6.1 | 34.8 | 2.0 | 4.7 | 3.5 | -23.4 | 4.6 | 42.2 | 0.1 | 2 |
| LP401−49 | 23.0967 | 23.9667 | 0.24 | 108 | -7.2 | 13.3 | 51.4 | 3.7 | -58.5 | 7.2 | -57.6 | 10.6 | 96.8 | 0.1 | 3 |
| LP933−66 | 23.1594 | -27.6267 | 0.21 | 98 | 3.6 | 7.2 | 42.8 | 2.1 | -41.5 | 4.0 | -35.0 | 5.6 | 69.1 | 0.1 | 3 |
| LP522−35 | 23.3000 | 12.7000 | 0.18 | 72 | 11.6 | 8.9 | 42.9 | 1.8 | -11.6 | 4.5 | -22.1 | 7.5 | 49.7 | 0.1 | 3 |
| LP762−53 | 23.3089 | -13.7333 | 0.20 | 150 | -1.2 | 10.2 | -6.1 | 2.1 | -63.5 | 5.2 | -27.5 | 8.5 | 69.5 | 0.1 | 1 |
| LP582−42 | 23.3250 | 09.5000 | 0.19 | 225 | 9.9 | 8.5 | -82.2 | 1.6 | -20.6 | 4.3 | -27.8 | 7.2 | 89.2 | 0.1 | 3 |
| G275−B16B | 23.3917 | -24.1817 | 0.06 | 175 | 33.9 | 21.1 | -51.9 | 5.1 | -100.4 | 11.5 | -50.1 | 17.0 | 123.6 | 0.1 | 3 |
| LP77−37A | 23.5717 | 64.6217 | 0.21 | 114 | 19.3 | 8.4 | 50.6 | 3.7 | -15.7 | 5.9 | -53.4 | 4.7 | 75.2 | 0.1 | 2 |
| LP463−27 | 23.6067 | 20.7500 | 0.33 | 58 | 32.5 | 7.3 | 37.7 | 1.5 | 10.0 | 3.9 | -20.9 | 6.0 | 44.3 | 0.1 | 1 |
| LP191−9 | 23.6892 | 47.1500 | 0.31 | 94 | 14.7 | 4.2 | 79.8 | 1.5 | -39.6 | 2.7 | -42.3 | 2.9 | 98.6 | 0.0 | 2 |
| LP347−5 | 23.6900 | 32.2700 | 0.24 | 256 | 15.7 | 3.4 | -12.5 | 0.9 | 3.7 | 2.0 | -14.1 | 2.6 | 19.2 | 0.1 | 3 |
| G273−B15A | 23.6958 | -16.4583 | 0.14 | 210 | 25.5 | 2.3 | -55.2 | 0.4 | -32.1 | 1.2 | -33.4 | 1.9 | 72.0 | 0.0 | 3 |
| LP935−14 | 23.7433 | -26.6650 | 0.36 | 255 | 49.6 | 5.7 | -91.1 | 1.3 | 7.2 | 3.2 | -37.8 | 4.6 | 98.9 | 0.0 | 3 |
| LP577−72 | 23.8586 | -33.5467 | 0.50 | 217 | 40.8 | ⋯ | -61.7 | ⋯ | -34.4 | ⋯ | -36.4 | ⋯ | 79.4 | ⋯ | 3 |
| LP524−35 | 23.9033 | 05.3833 | 0.21 | 69 | 31.7 | 8.3 | 55.0 | 0.7 | -3.8 | 4.1 | -33.1 | 7.2 | 64.3 | 0.1 | 3 |
| LP348−20 | 23.9817 | 27.0500 | 0.11 | 106 | 17.9 | 8.9 | 40.1 | 2.0 | -31.5 | 4.9 | -41.8 | 7.1 | 65.9 | 0.1 | 3 |

Silvestri et al.

TABLE 5 — *Continued*

| Identifier (dM) (1) | R.A. (B1950) (2) | Decl. (B1950) (3) | $\mu$ ($''$/yr) (4) | $\Theta$ (deg) (5) | $v_r$ (km/s) (6) | $\sigma_{v_r}$ (km/s) (7) | $U$ (km/s) (8) | $\sigma_U$ (km/s) (9) | $V$ (km/s) (10) | $\sigma_V$ (km/s) (11) | $W$ (km/s) (12) | $\sigma_W$ (km/s) (13) | S (k |
|---|---|---|---|---|---|---|---|---|---|---|---|---|---|

REFERENCES. — (1) dMe Stars; (2) dM(e) Stars; (3) dM Stars; (4) $V$ and $M_V$ are from the WD companion.

NOTE. — Units of right ascension are hours, and units of declination are degrees.

[a] Stellar halo white dwarf candidate.
[b] M dwarf has close (eclipsing) companion.